About Fourier optics

Éric Thiébaut

January 8, 2024

These notes are my attempt to collect the equations for numerical modeling of optical systems by physical optics propagation (POP). I tried to provide consistent results with a unified and readable notation[1], with demonstrations and, at least, the hypotheses that must hold.

Contents

[1] of course this is highly subjective

1 Theory of scalar waves propagation

1.1 From Maxwell equations to Helmholtz equation

This part is based on the book of **?**. In a medium with **no free charges**, Maxwell equations yield:

$$\nabla^2 \boldsymbol{U} + 2\,\nabla(\boldsymbol{U} \cdot \nabla \log n) = \frac{n^2}{c^2}\,\frac{\partial^2 \boldsymbol{U}}{\partial t^2}. \tag{1}$$

where $\boldsymbol{U} \in \mathbb{R}^3$ is either the electric field or the magnetic field as a function of space and time, n is the refractive index of the medium, c is the light speed in vacuum, t is the time, ∇ denotes spatial derivative, and ∇^2 is the Laplacian operator.

In an **homogeneous medium**, $\nabla \log n = 0$ and Eq. (1) simplifies to:

$$\nabla^2 \boldsymbol{U} = \frac{n^2}{c^2}\,\frac{\partial^2 \boldsymbol{U}}{\partial t^2} \tag{2}$$

which holds separately for the Cartesian components of $\boldsymbol{U}$ because the Laplacian of the vector field $\boldsymbol{U}$ writes:

$$\nabla^2 \boldsymbol{U} = (\nabla^2 U_x)\,\boldsymbol{e}_x + (\nabla^2 U_y)\,\boldsymbol{e}_y + (\nabla^2 U_z)\,\boldsymbol{e}_z \tag{3}$$

where (U_x, U_y, U_z) are the Cartesian components of $\boldsymbol{U}$ while $\boldsymbol{e}_x$, $\boldsymbol{e}_y$, and $\boldsymbol{e}_z$ are unit vectors along the corresponding Cartesian axes. Hence, the propagation equation simply writes:

$$\nabla^2 U(\boldsymbol{r}, t) = \frac{n^2}{c^2}\,\frac{\partial^2 U(\boldsymbol{r}, t)}{\partial t^2} \tag{4}$$

for any Cartesian component $U(\boldsymbol{r}, t) = U_x$, U_y, or U_z of $\boldsymbol{U}$. In the **scalar field theory**, the propagation of the field $\boldsymbol{U}$ is reduced to that of the component $U(\boldsymbol{r}, t)$. Working with $U(\boldsymbol{r}, t)$ is much simpler but is an approximation. In an inhomogeneous medium, the term $\nabla\big(\boldsymbol{U} \cdot \nabla \log n\big)$ introduces some coupling between the components of the field $\boldsymbol{U}$. Even though the medium is homogeneous, at close distances (a few wavelengths) of the edges of diffracting material, the coupling between the electric and magnetic fields and between their components cannot be neglected.

For a **monochromatic** electromagnetic wave, the scalar field is a separable function of the position $\boldsymbol{r}$ and of the time t which can be expressed as:

$$\boxed{U(\boldsymbol{r},t) = \mathrm{Re}\Big(u(\boldsymbol{r})\,\mathrm{e}^{-\mathrm{i}\,2\,\pi\,\nu\,t}\Big)} \tag{5}$$

with $\nu > 0$ the temporal frequency and where $u(\boldsymbol{r}) \in \mathbb{C}$ is a scalar field, called the **complex amplitude**, that only depends on the position $\boldsymbol{r}$. Thanks to this factorization, the time dependency in Eq. (4) can be dropped to yield the so-called **Helmholtz equation** for the propagation of $u(\boldsymbol{r})$:

$$\boxed{(\nabla^2 + k^2)\,u(\boldsymbol{r}) = 0} \tag{6}$$

with $k = 2\,\pi\,n\,\nu/c = 2\,\pi/\lambda$ the wave-number, $\lambda = c/(n\,\nu)$ the wavelength in the medium, and $\nabla^2 u = \partial^2 u/\partial x^2 + \partial^2 u/\partial y^2 + \partial^2 u/\partial z^2$ the Laplacian of u.

Two important specific solutions to the Helmholtz equation are described next, the plane and spherical waves, before considering more general solutions.

Plane wave.

With the convention in Eq. (5), the field produced by a plane wave writes:

$$U(\boldsymbol{r},t) = a\,\mathrm{Re}\Big(\mathrm{e}^{\mathrm{i}\,\boldsymbol{k}\cdot\boldsymbol{r} - \mathrm{i}\,2\,\pi\,\nu\,t}\Big) \tag{7}$$

with $a = U(\boldsymbol{0},0)$ and $\boldsymbol{k} = (k_x, k_y, k_z)$ the wave vector of amplitude $\|\boldsymbol{k}\| = k$ and whose direction is that of the propagation of the wave. The corresponding complex amplitude is:

$$u(\boldsymbol{r}) = a\,\mathrm{e}^{\mathrm{i}\,\boldsymbol{k}\cdot\boldsymbol{r}}, \tag{8}$$

whose Laplacian is:

$$\nabla^2 u(\boldsymbol{r}) = -\big(k_x^2 + k_y^2 + k_z^2\big)\,a\,\mathrm{e}^{\mathrm{i}\,\boldsymbol{k}\cdot\boldsymbol{r}} = -k^2\,u(\boldsymbol{r}) \tag{9}$$

hence a plane wave is solution of the Helmholtz equation (6).

Spherical wave.

With the convention in Eq. (5), the field produced by a spherical wave writes:

$$U(\boldsymbol{r},t) = a\,\mathrm{Re}\left(\frac{\mathrm{e}^{\mathrm{i}\,k\cdot\|\boldsymbol{r}-\boldsymbol{r}_0\| - \mathrm{i}\,2\,\pi\,\nu\,t}}{\|\boldsymbol{r}-\boldsymbol{r}_0\|}\right) \tag{10}$$

for some constant a and with $\boldsymbol{r}_0 = (x_0, y_0, z_0)$ the origin of the spherical wave. The factor in $1/\|\boldsymbol{r}-\boldsymbol{r}_0\|$ is to account for the dilution of the power with the radius of the sphere. Note that the expression is singular in $\boldsymbol{r} = \boldsymbol{r}_0$ where the field is not defined. The complex amplitude of the spherical wave is:

$$u(\boldsymbol{r}) = \frac{a}{\|\boldsymbol{r} - \boldsymbol{r}_0\|} \, \mathrm{e}^{\mathrm{i}\, k \cdot \|\boldsymbol{r} - \boldsymbol{r}_0\|}. \tag{11}$$

The derivatives in x of $u(\boldsymbol{r})$ with $\boldsymbol{r} = (x, y, z)$ are:

$$\frac{\partial u(\boldsymbol{r})}{\partial x} = \left(\frac{\mathrm{i}\, k}{\|\boldsymbol{r} - \boldsymbol{r}_0\|} - \frac{1}{\|\boldsymbol{r} - \boldsymbol{r}_0\|^2} \right) (x - x_0)\, u(\boldsymbol{r}), \tag{12}$$

$$\begin{aligned} \frac{\partial^2 u(\boldsymbol{r})}{\partial x^2} = \Bigg(& \frac{\mathrm{i}\, k}{\|\boldsymbol{r} - \boldsymbol{r}_0\|} - \frac{3\, \mathrm{i}\, k\, (x - x_0)^2}{\|\boldsymbol{r} - \boldsymbol{r}_0\|^3} - \frac{k^2\, (x - x_0)^2}{\|\boldsymbol{r} - \boldsymbol{r}_0\|^2} \\ & - \frac{1}{\|\boldsymbol{r} - \boldsymbol{r}_0\|^2} + \frac{3\, (x - x_0)^2}{\|\boldsymbol{r} - \boldsymbol{r}_0\|^4} \Bigg)\, u(\boldsymbol{r}), \end{aligned} \tag{13}$$

and similar expressions for the derivatives in y and z. Combining the second derivatives yields:

$$\nabla^2 u(\boldsymbol{r}) = -k^2\, u(\boldsymbol{r}) \tag{14}$$

hence a spherical wave is solution of the Helmholtz equation (6).

1.2 Diffraction by a surface

To determine the field $u(\boldsymbol{r}_1)$ at position $\boldsymbol{r}_1$ caused by given sources and using the Helmholtz equation (6), boundary conditions are needed. To that end, we may assume known the field at a closed surface Σ_0 such that all considered sources are inside the volume delimited by Σ_0 while $\boldsymbol{r}_1$ is outside this volume. Σ_0 may also be an infinite surface splitting the space in two with the sources on one side and $\boldsymbol{r}_1$ on the other side. Solving the Helmholtz equation for $u(\boldsymbol{r}_1)$ with such boundary conditions amounts to propagating the field from Σ_0 to $\boldsymbol{r}_1$. All considered sources being *behind* Σ_0 from the point of view of $\boldsymbol{r}_1$ and the Helmholtz equation being linear in the field at $u(\boldsymbol{r})$, the resulting field $\boldsymbol{r}_1$ must be a linear combination of all contributions from the *emitting surface* Σ_0:

$$u(\boldsymbol{r}_1) = \iint_{\boldsymbol{r}_0 \in \Sigma_0} h(\boldsymbol{r}_1, \boldsymbol{r}_0)\, u(\boldsymbol{r}_0)\, \mathrm{d}^2\Sigma_0, \tag{15}$$

where $h(\boldsymbol{r}_1, \boldsymbol{r}_0)$ is a **propagation kernel**.

1.3 Diffraction by a planar surface

Many simplifications occur if Σ_0 is a planar surface. If this is not the case, Kirchhoff diffraction equation can still be used (?) but is really not suitable for fast computations. In the following, we develop the theory for a wave diffracted by a planar surface. This amounts to deal with the **angular spectrum** for which solutions to the Helmholtz equation are quite easy to compute. Without demonstrating it, a solution for the field $u(\boldsymbol{r})$ provided by the type I **Rayleigh-Sommerfeld diffraction integral** is presented next for comparison.

1.3.1 Planar diffraction seen as a convolution

We consider the case where Σ_0 is an infinite plane and, without loss of generality, define the z-axis of the Cartesian coordinate system to be perpendicular to Σ_0 and oriented so that z increases as the waves physically propagate. In other words, the wave vector $\boldsymbol{k} = (k_x, k_y, k_z)$ of any propagating wave is such that $k_z > 0$. Since the space between Σ_0 and $\boldsymbol{r}_1$ is homogeneous and devoid of sources, propagation between $\boldsymbol{r}_0 \in \Sigma_0$ and $\boldsymbol{r}_1$ shall only depend on the relative position $\boldsymbol{r}_1 - \boldsymbol{r}_0$. In other words, the propagation kernel must be **shift-invariant** and Eq. (15) becomes:

$$u(\boldsymbol{r}_1) = \iint h(\boldsymbol{r}_1 - \boldsymbol{r}_0)\, u(\boldsymbol{r}_0)\, \mathrm{d}x_0\, \mathrm{d}y_0, \tag{16}$$

where (x_0, y_0, z_0) are the Cartesian coordinates of $\boldsymbol{r}_0$. At this point, it is useful to introduce:

$$u_z(\boldsymbol{x}) = u_z(x, y) \equiv u(x, y, z) \tag{17}$$

to express the field $u(\boldsymbol{r})$ in a **transverse plane** of the z-axis as a two-dimensional function of $\boldsymbol{x} = (x, y)$, the lateral position in this plane. Hereinafter, this notation will be used to emphasize that a function in a transverse plane at given z is considered. Using the same convention for the propagation kernel, Eq. (16) writes:

$$u_{z_1}(\boldsymbol{x}_1) = \iint h_{z_1 - z_0}(\boldsymbol{x}_1 - \boldsymbol{x}_0)\, u_{z_0}(\boldsymbol{x}_0)\, \mathrm{d}\boldsymbol{x}_0. \tag{18}$$

In words, the fields diffracted by a transverse plane is the **two-dimensional convolution** of the field u_{z_0} in the transverse plane at z_0 by a shift-invariant propagation kernel $h_{z_1 - z_0}(\boldsymbol{x})$ between this plane and the transverse plane at z_1.

1.3.2 The angular spectrum solution

The fact that the diffraction by a planar surface writes as a convolution in the transverse plane suggests to take the two-dimensional Fourier transform of the complex amplitude $u_z(\boldsymbol{x})$ in the transverse plane at position z:

$$\widetilde{u}_z(\boldsymbol{\alpha}) = \iint u_z(\boldsymbol{x})\, \mathrm{e}^{-\mathrm{i}\, 2\, \pi\, \boldsymbol{\alpha} \cdot \boldsymbol{x}}\, \mathrm{d}\boldsymbol{x} \tag{19}$$

with $\boldsymbol{\alpha} = (\alpha, \beta)$ the Fourier spatial frequency conjugate to the position $\boldsymbol{x} = (x, y)$ in the transverse plane. The inverse Fourier transform writes:

$$u_z(\boldsymbol{x}) = \iint \widetilde{u}_z(\boldsymbol{\alpha})\, \mathrm{e}^{+\mathrm{i}\, 2\, \pi\, \boldsymbol{\alpha} \cdot \boldsymbol{x}}\, \mathrm{d}\boldsymbol{\alpha}. \tag{20}$$

Taking the two-dimensional Fourier transform of both sides of Eq. (18), the propagation of the Fourier transform of the field from the transverse plane at z_0 to the

Notation	Description
n	Refractive index of the medium
c	Propagation speed in the void
ν	Temporal frequency of wave
$\lambda = c/(n\,\nu)$	Wavelength in the medium
$k = 2\,\pi/\lambda$	Wave number
$\boldsymbol{k} = (k_x, k_y, k_z)$	Wave vector (with $k_z > 0$)
$\boldsymbol{r} = (x, y, z)$	Position in 3-dimensional space
$\boldsymbol{x} = (x, y)$	Lateral position in a transverse plane
$\boldsymbol{\alpha} = (\alpha, \beta)$	Spatial frequency
$u_z(\boldsymbol{x}) = u_z(x, y) = u(x, y, z)$	Field in a transverse plane
$\widetilde{u}_z(\boldsymbol{\alpha}) = \widetilde{u}_z(\alpha, \beta)$	Angular spectrum, Fourier transform of $u_z(\boldsymbol{x})$

Table 1: Notations. All coordinates are Cartesian coordinates with the convention that the z-axis is oriented so that z increases as the waves physically propagate.

transverse plane at z_1 simplifies to:

$$\boxed{\widetilde{u}_{z_1}(\boldsymbol{\alpha}) = \widetilde{h}_{z_1 - z_0}(\boldsymbol{\alpha})\,\widetilde{u}_{z_0}(\boldsymbol{\alpha})} \tag{21}$$

with $\widetilde{h}_{\Delta z}(\boldsymbol{\alpha})$ the *propagation transfer function*, that is the Fourier transform of $h_{\Delta z}(\boldsymbol{x})$, the planar propagation kernel between transverse planes separated by Δz.

A number of necessary properties can be inferred without knowing the exact expression of the propagation transfer function $\widetilde{h}_{\Delta z}(\boldsymbol{\alpha})$:

- **No propagation.** If $z_1 = z_0$, the field shall remain unchanged, hence necessarily:
$$\widetilde{h}_0(\boldsymbol{\alpha}) = 1, \quad \forall \boldsymbol{\alpha}. \tag{22}$$

- **Successive propagation steps.** We expect that propagation can be split in successive propagation steps with the same result. For this property to hold, it is sufficient that propagation along the z-axis by Δz_1 and then by Δz_2 be the same as propagation by $\Delta z_1 + \Delta z_2$ whatever Δz_1 and Δz_2. In other words:
$$\widetilde{h}_{\Delta z_1}(\boldsymbol{\alpha})\,\widetilde{h}_{\Delta z_2}(\boldsymbol{\alpha}) = \widetilde{h}_{\Delta z_1 + \Delta z_2}(\boldsymbol{\alpha}), \quad \forall \boldsymbol{\alpha}, \Delta z_1, \Delta z_2. \tag{23}$$

- **Reverse propagation.** Ignoring possible divisions by zero, the propagation in Eq. (21) can be mathematically inverted to recover the Fourier transform of the field in the transverse plane at z_0 given the Fourier transform of the field in the transverse plane at z_1:
$$\widetilde{u}_{z_0}(\boldsymbol{\alpha}) = \frac{\widetilde{u}_{z_1}(\boldsymbol{\alpha})}{\widetilde{h}_{z_1 - z_0}(\boldsymbol{\alpha})}.$$
Besides, just exchanging z_0 and z_1 in Eq. (21) yields:
$$\widetilde{u}_{z_0}(\boldsymbol{\alpha}) = \widetilde{u}_{z_1}(\boldsymbol{\alpha})\,\widetilde{h}_{z_0 - z_1}(\boldsymbol{\alpha}).$$

These two relations must hold whatever the propagated field and the transverse positions z_0 and z_1, hence necessarily:

$$\widetilde{h}_{-\Delta z}(\boldsymbol{\alpha}) = \frac{1}{\widetilde{h}_{\Delta z}(\boldsymbol{\alpha})}, \quad \forall \boldsymbol{\alpha}, \Delta z. \tag{24}$$

We note that, if the propagation transfer function takes the form:

$$\widetilde{h}_z(\boldsymbol{\alpha}) = \mathrm{e}^{z\,\psi(\boldsymbol{\alpha})} \tag{25}$$

for any function $\psi\colon \mathbb{R}^2 \to \mathbb{C}$, then the properties (22), (23), and (24) hold as can be easily verified. Is there any other possibilities?

The expression of $\widetilde{h}_z(\boldsymbol{\alpha})$ can be obtained by solving the Helmholtz equation for the Fourier transform of the field. The following spatial derivatives of the field $u_z(\boldsymbol{x})$ can be obtained from Eq. (20) with $\boldsymbol{\alpha} = (\alpha, \beta)$ and $\boldsymbol{x} = (x, y)$:

$$\frac{\partial^m u_z(x,y)}{\partial x^m} = (i\,2\,\pi)^m \iint \widetilde{u}_z(\alpha,\beta)\,\alpha^m\,\mathrm{e}^{+\mathrm{i}\,2\,\pi\,(\alpha\,x+\beta\,y)}\,\mathrm{d}\alpha\,\mathrm{d}\beta, \tag{26}$$

$$\frac{\partial^m u_z(x,y)}{\partial y^m} = (i\,2\,\pi)^m \iint \widetilde{u}_z(\alpha,\beta)\,\beta^m\,\mathrm{e}^{+\mathrm{i}\,2\,\pi\,(\alpha\,x+\beta\,y)}\,\mathrm{d}\alpha\,\mathrm{d}\beta, \tag{27}$$

$$\frac{\partial^m u_z(x,y)}{\partial z^m} = \iint \frac{\partial^m \widetilde{u}_z(\alpha,\beta)}{\partial z^m}\,\mathrm{e}^{+\mathrm{i}\,2\,\pi\,(\alpha\,x+\beta\,y)}\,\mathrm{d}\alpha\,\mathrm{d}\beta, \tag{28}$$

for any $m \in \mathbb{N}$. Using these expressions (with $m = 2$) and applying the Helmholtz equation (6) to the field $u_z(\boldsymbol{x})$ given in Eq. (20) yields the equation of propagation for the Fourier transform of the field:

$$k^2\left[1 - \lambda^2\,\|\boldsymbol{\alpha}\|^2\right]\widetilde{u}_z(\boldsymbol{\alpha}) + \frac{\partial^2 \widetilde{u}_z(\boldsymbol{\alpha})}{\partial z^2} = 0. \tag{29}$$

Remarkably, the Helmholtz equation is much simpler for the Fourier transform of the field than for the field because it only presents derivatives along z. In effect, by using the Fourier transform, the partial derivatives along the lateral coordinates have been replaced by simple multiplications by powers of the spatial frequencies.

Integrating Eq. (29) for z from z_0 to z_1 gives the following general solution for the Fourier transform of the field in the transverse plane at z_1:

$$\widetilde{u}_{z_1}(\boldsymbol{\alpha}) = \begin{cases} a_+(\boldsymbol{\alpha})\,\mathrm{e}^{+\mathrm{i}\,k\,\Delta z\,\sqrt{1-\lambda^2\,\|\boldsymbol{\alpha}\|^2}} \\ \quad + a_-(\boldsymbol{\alpha})\,\mathrm{e}^{-\mathrm{i}\,k\,\Delta z\,\sqrt{1-\lambda^2\,\|\boldsymbol{\alpha}\|^2}} & \text{if } \lambda\,\|\boldsymbol{\alpha}\| \le 1, \\ a_+(\boldsymbol{\alpha})\,\mathrm{e}^{+k\,\Delta z\,\sqrt{\lambda^2\,\|\boldsymbol{\alpha}\|^2-1}} \\ \quad + a_-(\boldsymbol{\alpha})\,\mathrm{e}^{-k\,\Delta z\,\sqrt{\lambda^2\,\|\boldsymbol{\alpha}\|^2-1}} & \text{if } \lambda\,\|\boldsymbol{\alpha}\| > 1, \end{cases} \tag{30}$$

with $\Delta z = z_1 - z_0$ and where $a_+(\boldsymbol{\alpha})$ and $a_-(\boldsymbol{\alpha})$ are functions to be determined by the boundary conditions. Taking $z_1 = z_0$ in both hand-sides of the general solution in Eq. (30) yields the boundary conditions at $z = z_0$:

$$a_+(\boldsymbol{\alpha}) + a_-(\boldsymbol{\alpha}) = \widetilde{u}_{z_0}(\boldsymbol{\alpha}). \tag{31}$$

According to our convention that z increases as the waves physically propagate, then:

- $\Delta z = z_1 - z_0 > 0$ corresponds to **forward propagation**, *i.e.* the wave is physically propagating from z_0 to $z_1 = z_0 + \Delta z$;
- $\Delta z < 0$ corresponds to **reverse propagation**.

To eliminate un-physical solutions, we consider the case of forward propagation, *i.e.* $\Delta z > 0$. There are two regimes to examine:

- If $\|\boldsymbol{\alpha}\| \leq 1/\lambda$, the convention in Eq. (5) implies that the phase of the propagating wave is increasing with the distance of propagation, hence $a_- = 0$ and, from Eq. (31), $a_+ = \widetilde{u}_{z_0}$. The solution then writes:
$$\widetilde{u}_{z_1}(\boldsymbol{\alpha}) = \widetilde{u}_{z_0}(\boldsymbol{\alpha})\, \mathrm{e}^{\mathrm{i}\, k\, \Delta z\, \sqrt{1-\lambda^2\, \|\boldsymbol{\alpha}\|^2}}. \tag{32}$$

- If $\|\boldsymbol{\alpha}\| > 1/\lambda$, the amplitude of the wave must not increase with the distance of propagation, hence $a_+ = 0$ and, from Eq. (31), $a_- = \widetilde{u}_{z_0}$. The solution then writes:
$$\widetilde{u}_{z_1}(\boldsymbol{\alpha}) = \widetilde{u}_{z_0}(\boldsymbol{\alpha})\, \mathrm{e}^{-k\, \Delta z\, \sqrt{\lambda^2\, \|\boldsymbol{\alpha}\|^2 - 1}}. \tag{33}$$
This high frequencies regime corresponds to **evanescent waves** that are rapidly vanishing with the distance of propagation: no spatial frequencies higher than $1/\lambda$ are propagating.

Combining these solutions with Eq. (21), the transfer function implementing the propagation between transverse planes for the Fourier transform of the field writes:
$$\widetilde{h}_{\Delta z}(\boldsymbol{\alpha}) = \begin{cases} \exp\left(\mathrm{i}\, k\, \Delta z\, \sqrt{1 - \lambda^2\, \|\boldsymbol{\alpha}\|^2}\right) & \text{if } \|\boldsymbol{\alpha}\| \leq 1/\lambda, \\ \exp\left(-k\, \Delta z\, \sqrt{\lambda^2\, \|\boldsymbol{\alpha}\|^2 - 1}\right) & \text{if } \|\boldsymbol{\alpha}\| > 1/\lambda. \end{cases} \tag{34}$$

High-frequencies, *i.e.* $\|\boldsymbol{\alpha}\| > 1/\lambda$, which corresponds to evanescent waves can be neglected except for short propagation distances. A more synthetic expression of Eq. (34) is provided by:
$$\boxed{\widetilde{h}_{\Delta z}(\boldsymbol{\alpha}) = \exp\left(\mathrm{i}\, k\, \Delta z\, \sqrt{1 - \lambda^2\, \|\boldsymbol{\alpha}\|^2}\right)} \tag{35}$$
which holds for $\|\boldsymbol{\alpha}\| \leq 1/\lambda$ and for $\|\boldsymbol{\alpha}\| > 1/\lambda$ with the usual convention that $\sqrt{t} = \mathrm{i}\, \sqrt{-t}$ when $t < 0$.

The transfer function in Eq. (35) has the exponential form envisioned in Eq. (25), hence the properties (22), (23), and (24) do hold for $\widetilde{h}_{\Delta z}(\boldsymbol{\alpha})$. In particular, the reverse propagation property in Eq. (24) which means that the theory is consistent for forward ($\Delta z > 0$) and reverse ($\Delta z < 0$) propagation. The expression of the propagation transfer function in Eq. (35) is therefore valid whatever the sign of Δz. As shown later, this is not the case for the Rayleigh-Sommerfeld diffraction integral presented in Section 1.3.3.

Angular spectrum

Combining Eqs. (20), (21), and (35), the field in the transverse plane at position $z > 0$ knowing (the Fourier transform of) the field in the transverse plane at $z = 0$ writes:

$$\begin{aligned} u_z(\boldsymbol{x}) &= \iint \widetilde{u}_0(\boldsymbol{\alpha})\, \widetilde{h}_z(\boldsymbol{\alpha})\, \mathrm{e}^{+\mathrm{i}\, 2\,\pi\, \boldsymbol{\alpha}\cdot\boldsymbol{x}}\, \mathrm{d}\boldsymbol{\alpha} \\ &= \iint \widetilde{u}_0(\boldsymbol{\alpha})\, \mathrm{e}^{+\mathrm{i}\left(2\,\pi\, \boldsymbol{\alpha}\cdot\boldsymbol{x} + k\, z\, \sqrt{1-\lambda^2\, \|\boldsymbol{\alpha}\|^2}\right)}\, \mathrm{d}\boldsymbol{\alpha} \end{aligned} \tag{36}$$

which can be seen as the superposition of plane waves, see Eq. (8), weighted by $\widetilde{u}_0(\boldsymbol{\alpha})$ and whose wave vectors $\boldsymbol{k} = (k_x, k_y, k_z)$ are given by:

$$\begin{cases} \boldsymbol{k}_\perp = (k_x, k_y) = 2\,\pi\,(\alpha, \beta) = 2\,\pi\,\boldsymbol{\alpha} \\ k_z = k\,\sqrt{1 - \lambda^2\,\|\boldsymbol{\alpha}\|^2} \end{cases} \tag{37}$$

In this representation, the spatial frequencies multiplied by the wavelength, $\lambda\,\boldsymbol{\alpha}$, are the cosines of the angles of the wave vector $\boldsymbol{k}$ with the lateral unit vectors $\boldsymbol{e}_x$ and $\boldsymbol{e}_y$. For that reason, the Fourier spectrum $\widetilde{u}_z(\boldsymbol{\alpha})$ is called the **angular spectrum** of the field in the transverse plane at z. In Appendix A, the Helmholtz equation is solved assuming that the field is a superposition of plane waves. **?** propose another resolution of the Helmholtz equation directly based on the interpretation that the inverse Fourier transform of the angular spectrum, Eq. (20), is readily a superposition of plane waves for which the propagation is known, *cf.* Eq. (8).

1.3.3 Rayleigh-Sommerfeld diffraction

The field in the transverse plane at $z > 0$ caused by the propagation of the field in the the transverse plane at $z = 0$ can be computed by the (type I?) Rayleigh-Sommerfeld diffraction integral (**???**):

$$u_z(x, y) = \frac{-1}{2\,\pi} \iint u_0(x', y')\, \frac{\partial}{\partial z}\left(\frac{\mathrm{e}^{\mathrm{i}\,k\,r'}}{r'}\right) \mathrm{d}x'\, \mathrm{d}y' \tag{38}$$

where $r' = \sqrt{(x-x')^2 + (y-y')^2 + z^2}$ and for $z > 0$. Note that the term $\mathrm{e}^{\mathrm{i}\,k\,r'}/r'$ corresponds to a spherical wave emitted by a source at $(x', y', 0)$.

Rayleigh-Sommerfeld diffraction integral has the form expected by Eq. (15) with the propagation kernel:

$$\boxed{h_z(x, y) = \frac{-1}{2\,\pi}\, \frac{\partial}{\partial z}\left(\frac{\mathrm{e}^{\mathrm{i}\,k\,r}}{r}\right) = \frac{z\,\mathrm{e}^{\mathrm{i}\,k\,r}}{r^2}\left(\frac{1}{\mathrm{i}\,\lambda} + \frac{1}{2\,\pi\,r}\right)} \tag{39}$$

for $z > 0$ and with $r = \sqrt{x^2 + x^2 + z^2}$ the distance of propagation, and λ the wavelength in the propagation medium. As claimed before, this function is indeed shift-invariant. Note that the term $1/(2\,\pi\,r)$ accounts for evanescent waves and is negligible at propagating distances longer than a few wavelengths.

As rigorously proven by **?**, the inverse Fourier transform of the angular spectrum transfer function $\widetilde{h}_z(\boldsymbol{\alpha})$ given in Eq. (35) is the propagation kernel $h_z(\boldsymbol{x})$ given in Eq. (39) however for $z \geq 0$, that is for forward propagation.

1.4 Paraxial approximation: Fresnel diffraction

Fresnel diffraction is an approximation of the diffraction by a planar surface when the so-called **paraxial conditions** hold. These conditions are satisfied in the following cases (which are all equivalent):

- the high frequencies of the angular spectrum are negligible;
- the variations of the complex amplitude along the direction perpendicular to the surface can be well approximated by those of a plane wave;
- diffracted waves have small propagation angles with the normal to the diffracting surface.

Fresnel diffraction is important because the above conditions correspond to many common practical cases and because it yields equations that are well adapted to fast numeric computations (*i.e.* integrals can be evaluated by means of FFTs). The Fresnel approximation of the diffraction can be obtained from any of the above conditions. We start by the angular spectrum which (again) is the most straightforward and consistent path to follow. The other approaches are considered next.

1.4.1 The angular spectrum transfer function at low frequencies

If the angular spectrum $\widetilde{u}_z(\boldsymbol{\alpha})$ is only significant at low frequencies such that $\|\boldsymbol{\alpha}\| \ll 1/\lambda$, then, to apply the angular spectrum propagation in Eq. (21), it is sufficient to consider an approximation of the angular spectrum transfer function given by Eq. (35) in that regime:

$$\widetilde{h}_{\Delta z}(\boldsymbol{\alpha}) = \mathrm{e}^{\mathrm{i}\,k\,\Delta z\,\sqrt{1-\lambda^2\,\|\boldsymbol{\alpha}\|^2}} \underset{\|\boldsymbol{\alpha}\|\ll 1/\lambda}{\approx} \mathrm{e}^{\mathrm{i}\,k\,\Delta z\,\left[1-\frac{1}{2}\,\lambda^2\,\|\boldsymbol{\alpha}\|^2\right]}. \tag{40}$$

This yields the paraxial approximation of the angular spectrum propagation transfer function:

$$\boxed{\widetilde{h}_{\Delta z}(\boldsymbol{\alpha}) = \mathrm{e}^{\mathrm{i}\,\left(k-\pi\,\lambda\,\|\boldsymbol{\alpha}\|^2\right)\,\Delta z} \quad \text{for } \|\boldsymbol{\alpha}\| \ll 1/\lambda} \tag{41}$$

with λ the wavelength in the medium. It is worth noting that this transfer function has the exponential form given in Eq. (25), hence the properties (22), (23), and (24) do hold for the paraxial approximation of $\widetilde{h}_z(\boldsymbol{\alpha})$.

In order to derive a closed-form expression of the propagation kernel $h_z(\boldsymbol{x})$ in the paraxial conditions, we need to generalize the (inverse) Fourier transform of a two-dimensional Gaussian shaped function:

$$\boxed{\iint \mathrm{e}^{-\pi\, q\, \|\boldsymbol{x}\|^2}\, \mathrm{e}^{\pm \mathrm{i}\, 2\, \pi\, \boldsymbol{x}\cdot\boldsymbol{\alpha}}\, \mathrm{d}\boldsymbol{x} = \frac{\mathrm{e}^{-\frac{\pi}{q}\, \|\boldsymbol{\alpha}\|^2}}{q}} \tag{42}$$

which is also a Gaussian shaped function. Equation (42) holds for any $q > 0$. By analytic continuation, we assume that Eq. (42) also holds for any $q \in \mathbb{C}^\star$ such that $\mathrm{Re}(q) \geq 0$. In particular[2], taking $q = \mathrm{i}\, \rho$ with $\rho \in \mathbb{R}^\star$ in Eq. (42) yields the (inverse) Fourier transform of a two-dimensional quadratic phase factor:

$$\iint \mathrm{e}^{-\mathrm{i}\, \pi\, \rho\, \|\boldsymbol{x}\|^2}\, \mathrm{e}^{\pm \mathrm{i}\, 2\, \pi\, \boldsymbol{x}\cdot\boldsymbol{\alpha}}\, \mathrm{d}\boldsymbol{x} = \frac{\mathrm{e}^{\frac{\mathrm{i}\, \pi}{\rho}\, \|\boldsymbol{\alpha}\|^2}}{\mathrm{i}\, \rho} \tag{43}$$

which is also a quadratic phase factor. Using Eq. (43), the inverse Fourier transform of the propagation transfer function given in Eq. (41) can be computed to yield the propagation kernel in the paraxial approximation:

$$\boxed{h_{\Delta z}(\Delta\boldsymbol{x}) = \frac{\mathrm{e}^{\mathrm{i}\, k\, \Delta z}}{\mathrm{i}\, \lambda\, \Delta z}\, \mathrm{e}^{\frac{\mathrm{i}\, \pi\, \|\Delta\boldsymbol{x}\|^2}{\lambda\, \Delta z}} = \frac{\mathrm{e}^{\mathrm{i}\, k\, \Delta z}}{\mathrm{i}\, \lambda\, \Delta z}\, \mathrm{e}^{\frac{\mathrm{i}\, k\, \|\Delta\boldsymbol{x}\|^2}{2\, \Delta z}}} \tag{44}$$

As shown next, the condition $\|\boldsymbol{\alpha}\| \ll 1/\lambda$ for Eq. (41) is equivalent to $\|\Delta\boldsymbol{x}\| \ll |\Delta z|$ for Eq. (44). Propagation by this kernel implements **Fresnel diffraction**:

$$\boxed{u_{z_1}(\boldsymbol{x}_1) = \frac{\mathrm{e}^{\mathrm{i}\, k\, \Delta z}}{\mathrm{i}\, \lambda\, \Delta z} \iint u_{z_0}(\boldsymbol{x}_0)\, \mathrm{e}^{\frac{\mathrm{i}\, \pi\, \|\boldsymbol{x}_1 - \boldsymbol{x}_0\|^2}{\lambda\, \Delta z}}\, \mathrm{d}\boldsymbol{x}_0} \tag{45}$$

with $\Delta z = z_1 - z_0$.

1.4.2 Modulation of a plane carrier wave

The field $u(x, y, z)$ can be expressed as a modulation of a chosen carrier wave. Assuming that the carrier wave is a plane wave whose wave vector is $\boldsymbol{k} = k\, \boldsymbol{e}_z$, the field can be expressed as:

$$u(x, y, z) = a(x, y, z)\, \mathrm{e}^{\mathrm{i}\, k\, z}, \tag{46}$$

[2] The more general case of $q \in \mathbb{C}^\star$ such that $\mathrm{Re}(q) \geq 0$ is suitable to derive the equations of propagation for a Gaussian beam.

with $a(x, y, z)$ the modulation field. Using this above expression, the derivatives of $u(x, y, z)$ are:

$$\frac{\partial^2 u(x,y,z)}{\partial x^2} = \frac{\partial^2 a(x,y,z)}{\partial x^2}\, \mathrm{e}^{\mathrm{i}\,k\,z}, \tag{47}$$
$$\frac{\partial^2 u(x,y,z)}{\partial y^2} = \frac{\partial^2 a(x,y,z)}{\partial y^2}\, \mathrm{e}^{\mathrm{i}\,k\,z}, \tag{48}$$
$$\frac{\partial u(x,y,z)}{\partial z} = \left(\frac{\partial a(x,y,z)}{\partial z} + \mathrm{i}\,k\,a(x,y,z)\right) \mathrm{e}^{\mathrm{i}\,k\,z}, \tag{49}$$
$$\frac{\partial^2 u(x,y,z)}{\partial z^2} = \left(\frac{\partial^2 a(x,y,z)}{\partial z^2} + 2\,\mathrm{i}\,k\,\frac{\partial a(x,y,z)}{\partial z} - k^2\,a(x,y,z)\right) \mathrm{e}^{\mathrm{i}\,k\,z}. \tag{50}$$

Using Eqs. (47), (48), and (50), the Helmholtz equation (6) for the modulation field $a(x, y, z)$ writes:

$$\left(\underbrace{\frac{\partial^2}{\partial x^2} + \frac{\partial^2}{\partial y^2} + \frac{\partial^2}{\partial z^2}}_{\nabla^2} + 2\,\mathrm{i}\,k\,\frac{\partial}{\partial z}\right) a(x,y,z) = 0. \tag{51}$$

In the **paraxial approximation**, it is assumed that the carrier plane wave explains most of the variations of the field along z and thus that the second derivative of the modulation $a(x, y, z)$ in z is negligible compared to the term involving the first derivative:

$$\left|\frac{\partial^2 a}{\partial z^2}\right| \ll \left|2\,k\,\frac{\partial a}{\partial z}\right| \quad \Longrightarrow \quad \left(\underbrace{\frac{\partial^2}{\partial x^2} + \frac{\partial^2}{\partial y^2}}_{\nabla_\perp^2} + 2\,\mathrm{i}\,k\,\frac{\partial}{\partial z}\right) a(x,y,z) = 0, \tag{52}$$

which is the **paraxial wave equation** for the modulation field $a(x, y, z)$. Multiplying by $\exp(\mathrm{i}\,k\,z)$ and using Eq. (49), the paraxial wave equation for the field writes[3]:

$$\left(\underbrace{\frac{\partial^2}{\partial x^2} + \frac{\partial^2}{\partial y^2}}_{\nabla_\perp^2} + 2\,\mathrm{i}\,k\,\frac{\partial}{\partial z} - 2\,k^2\right) u(x,y,z) = 0. \tag{53}$$

Using the same notation as in Eq. (17) and the two-dimensional Fourier in a transverse plane and its inverse defined in Eqs. (19) and (20), the paraxial wave equation for the Fourier transform of the modulation field writes:

$$\frac{\partial \widetilde{a}_z(\boldsymbol{\alpha})}{\partial z} = -\mathrm{i}\,\pi\,\lambda\,\|\boldsymbol{\alpha}\|^2\,\widetilde{a}_z(\boldsymbol{\alpha}). \tag{54}$$

Integration of this equation for z from z_0 to $z_1 = z_0 + \Delta z$ yields:

$$\widetilde{a}_{z_1}(\boldsymbol{\alpha}) = \widetilde{a}_{z_0}(\boldsymbol{\alpha})\,\mathrm{e}^{-\mathrm{i}\,\pi\,\lambda\,\Delta z\,\|\boldsymbol{\alpha}\|^2}. \tag{55}$$

[3] in https://en.wikipedia.org/wiki/Helmholtz_equation#Paraxial_approximation a different solution is given without the k^2 term...

From Eq. (46) and by linearity of the transverse Fourier transform, it is easy to show that:

$$\widetilde{u}_z(\boldsymbol{\alpha}) = \widetilde{a}_z(\boldsymbol{\alpha})\,\mathrm{e}^{\mathrm{i}\,k\,z}, \tag{56}$$

and thus:

$$\widetilde{u}_{z_1}(\boldsymbol{\alpha}) = \widetilde{u}_{z_0}(\boldsymbol{\alpha})\,\mathrm{e}^{\mathrm{i}\,\left(k-\pi\,\lambda\,\|\boldsymbol{\alpha}\|^2\right)\,\Delta z}. \tag{57}$$

The transfer function in the above right-hand side is exactly the paraxial approximation of the angular spectrum propagation transfer function given in Eq. (41). Hence, the approximation of neglecting the second derivatives in z of the modulation field which leads to Eq. (52) is equivalent to the approximation $\sqrt{1-\|\lambda\,\boldsymbol{\alpha}\|^2} \approx 1 - \|\lambda\,\boldsymbol{\alpha}\|^2/2$ that holds at low frequencies such that $\|\boldsymbol{\alpha}\| \ll 1/\lambda$ and used to obtain Eq. (41) more directly.

1.4.3 From Rayleigh-Sommerfeld diffraction to Fresnel diffraction

Finally, it is interesting to derive an expression of the propagation kernel in paraxial conditions by approximating the Rayleigh-Sommerfeld propagation kernel h_z given in Eq. (39), hence neglecting evanescent waves, for small diffraction angles. For small diffraction angles, $\|\Delta\boldsymbol{x}\|$ is small compared to $|\Delta z|$ and the following series can be used to approximate r the propagation distance used in Eq. (39):

$$\begin{aligned} r &= \sqrt{\|\Delta\boldsymbol{x}\|^2 + \Delta z^2} \\ &= |\Delta z|\,\sqrt{1 + \|\Delta\boldsymbol{x}/\Delta z\|^2} \\ &= |\Delta z| + \frac{\|\Delta\boldsymbol{x}\|^2}{2\,|\Delta z|} - \frac{\|\Delta\boldsymbol{x}\|^4}{8\,|\Delta z|^3} + \frac{\|\Delta\boldsymbol{x}\|^6}{16\,|\Delta z|^5} - \ldots \end{aligned} \tag{58}$$

In the denominator of the right-hand side expression of Eq. (39), the first term of the series is sufficient but, in the complex exponential, at least the two first terms must be kept to account for the phase changes with the lateral position $\boldsymbol{x} = (x, y)$. More specifically, the third and subsequent terms of the series can be neglected in the $\mathrm{e}^{\mathrm{i}\,k\,r}$ term if the following condition holds:

$$\frac{\|\Delta\boldsymbol{x}\|^4}{8\,|\Delta z|^3} \ll \lambda \quad \Longleftrightarrow \quad \|\Delta\boldsymbol{x}\| \ll \left(8\,\lambda\,|\Delta z|^3\right)^{1/4}. \tag{59}$$

which is another expression of the **paraxial conditions**[4]. If these conditions hold, the Rayleigh-Sommerfeld propagation kernel can be approximated by:

$$h_{\Delta z}(\Delta\boldsymbol{x}) \approx \frac{\exp\!\left(\mathrm{i}\,k\left[|\Delta z| + \frac{\|\Delta\boldsymbol{x}\|^2}{2\,|\Delta z|}\right]\right)}{\mathrm{i}\,\lambda\,\Delta z}$$

whose right-hand-side is the Fresnel propagation kernel given in Eq. (44) except that Δz is replaced by $|\Delta z|$ in the exponential function. The two expressions are only identical for $\Delta z \geq 0$ that is for *forward propagation*. Rayleigh-Sommerfeld theory is not suitable for *reverse propagation*.

[4] For a wavelength $\lambda = 500\,\mathrm{nm}$, the paraxial conditions in Eq. (59) correspond to a region of about 1 mm in radius at a propagation distance $\Delta z = 1$ cm.

1.4.4 Alternative formulation of Fresnel diffraction integral

The Fresnel diffraction integral in Eq. (45) has the form of a convolution which can be computed by 2 Fourier transforms using the expression of the propagation transfer function (or 3 Fourier transforms if the expression of the propagation kernel is used instead). As shown next, the Fresnel diffraction integral can also be computed by a single Fourier transform.

Introducing the quadratic phase factor:

$$\mathcal{Q}_\rho(\boldsymbol{x}) = \exp\Bigl(\mathrm{i}\,\pi\,\rho\,\|\boldsymbol{x}\|^2\Bigr) \tag{60}$$

and developping the term $\|\boldsymbol{x}_1 - \boldsymbol{x}_0\|^2$ in the Fresnel propagation kernel given by Eq. (44), the field in the transverse plane at z_1 can be written as:

$$u_{z_1}(\boldsymbol{x}_1) = \frac{\mathrm{e}^{\mathrm{i}\,k\,\Delta z}}{\mathrm{i}\,\lambda\,\Delta z}\,\mathcal{Q}_{\frac{1}{\lambda\,\Delta z}}(\boldsymbol{x}_1) \iint \Bigl[u_{z_0}(\boldsymbol{x}_0)\,\mathcal{Q}_{\frac{1}{\lambda\,\Delta z}}(\boldsymbol{x}_0)\Bigr]\,\mathrm{e}^{-\frac{\mathrm{i}\,2\,\pi}{\lambda\,\Delta z}\,\boldsymbol{x}_1\cdot\boldsymbol{x}_0}\,\mathrm{d}\boldsymbol{x}_0 \tag{61}$$

with $\Delta z = z_1 - z_0$. Note that the two-dimensional integral is the Fourier transform[5] of the term inside the square brackets at the *frequency* $\boldsymbol{\alpha} = \boldsymbol{x}_1/(\lambda\,|\Delta z|)$. This formula and the angular spectrum are two possible methods to numerically compute the propagation by means of fast Fourier transforms (FFTs).

1.4.5 Planar wave in the paraxial approximation.

In the paraxial approximation, the wave-vector $\boldsymbol{k} = (k_x, k_y, k_z)$ of a planar wave is such that $|k_x| \ll |k_z|$ and $|k_y| \ll |k_z|$. Hence and because of the choice of the orientation of the z-axis which implies that $k_z > 0$, $k_z \approx k$. Using the planar wave decomposition of Eq. (36), a planar wave

$$u_z(x, y) \propto \mathrm{e}^{\mathrm{i}\,\left(\boldsymbol{k}_\perp\cdot\boldsymbol{x} + z\,\sqrt{k^2 - \|\boldsymbol{k}_\perp\|^2}\right)} \approx \mathrm{e}^{\mathrm{i}\,k\,z}\,\mathrm{e}^{\mathrm{i}\,\boldsymbol{k}_\perp\cdot\boldsymbol{x}} \tag{62}$$

with $\boldsymbol{k}_\perp = (k_x, k_y) = 2\,\pi\,\boldsymbol{\alpha}$ where $\boldsymbol{\alpha}$ is the spatial frequency of the angular spectrum of the planar wave.

1.4.6 Spherical wave in the paraxial approximation.

In the paraxial approximation, a spherical wave originating from $\boldsymbol{r}_0 = (x_0, y_0, z_0)$ becomes:

$$u_z(x, y) \propto \frac{\mathrm{e}^{\mathrm{i}\,k\,\|\boldsymbol{r}-\boldsymbol{r}_0\|}}{\|\boldsymbol{r}-\boldsymbol{r}_0\|} = \frac{\mathrm{e}^{\mathrm{i}\,k\,\sqrt{\|\boldsymbol{x}-\boldsymbol{x}_0\|^2 + \Delta z^2}}}{\sqrt{\|\boldsymbol{x}-\boldsymbol{x}_0\|^2 + \Delta z^2}} \approx \frac{\mathrm{e}^{\mathrm{i}\,k\,\left(|\Delta z| + \frac{\|\boldsymbol{x}-\boldsymbol{x}_0\|^2}{2\,|\Delta z|}\right)}}{|\Delta z|} \tag{63}$$

with $\boldsymbol{r} = (x, y, z)$, $\Delta z = z - z_0$, $\boldsymbol{x} = (x, y)$, and $\boldsymbol{x}_0 = (x_0, y_0)$. Note that, the right-hand side of Eq. (63) is equal to $(-\mathrm{i}/\lambda)\,h_{|\Delta z|}(\boldsymbol{x})$ with $h_{\Delta z}$ the Fresnel propagation kernel given in Eq. (44).

[5] if $\Delta z > 0$, inverse Fourier transform if $\Delta z < 0$

1.4.7 Gaussian beam in the paraxial approximation

1.5 Fraunhofer diffraction

2 Propagation methods

Equipped with the equations of propagation, we can now consider how to use them for modeling optical propagation. There are several possible fast methods[6] to propagate the field:

- **Propagation by discrete convolution.** This method consists in approximating the diffraction integral in Eq. (18) by a discrete convolution computed by means of 3 FFTs and by sampling either the non-paraxial (Rayleigh-Sommerfeld) or paraxial (Fresnel) propagation kernels. This method is developed in Section 2.2.

- **Propagation by the transfer function.** This method is similar to the propagation by convolution except that the propagation transfer function is directly sampled instead of being computed by the DFT of the sampled propagation kernel. Either the non-paraxial (Rayleigh-Sommerfeld) or the paraxial (Fresnel) propagation transfer functions may be used. This method costs 2 FFTs.

- **Propagation by the Fresnel transform.** Expanding the quadratic phase factor in the Fresnel propagation kernel in Eq. (44), the Fresnel diffraction integral may be rewritten as in Eq. (61) where the integral can be computed by a single Fourier transform. Hence, this method costs 1 FFT.

- **Propagation by the fractional Fourier transform.** This method, also called the 2-step Fresnel transform, amounts to performing two consecutive propagations by the Fresnel transform and hence costs 2 FFTs.

- **Fraunhofer propagation.** This method can be applied if the Fraunhofer conditions hold. For example, to propagate the field at a thin lens to the back focal plane of the lens. Fraunhofer propagation is done by a single FFT.

The computational cost is not the only thing to consider with these methods: there are also aliasing, sampling, and range issues. The convolution-based methods impose to keep the same sampling step in the input and output transverse planes, while the Fresnel transform imposes a magnification of the sampling step which depends on the propagation distance. In the 2-step Fresnel transform, there is some freedom for choosing the sampling step in the output transverse plane. Under the paraxial approximation, it is also possible to rewrite the convolution integral to have a sampling step in the output transverse plane that is not the same as in the input transverse plane. This latter method is exactly equivalent to a 2-step Fresnel transform.

2.1 Sampling

For numerical computations, the continuous functions of the lateral position and spatial frequency are sampled on a regular Cartesian grid. We further assume that the

[6] using FFTs for efficiency

number of samples and the sampling steps are the same along the 2 dimensions of the sampled transverse plane. This subsection briefly introduces the relations between the sampled field and the sampled angular spectrum based on the properties developed in Appendix B.

Following our assumptions, the transverse plane is considered to be sampled on a $N \times N$ grid with step δx at positions:

$$\boldsymbol{x}[\boldsymbol{j}] = \delta x \times \boldsymbol{j} \tag{64}$$

for all $\boldsymbol{j} \in \mathbb{J}^2$ and where (following FFT conventions):

$$\mathbb{J} = \begin{cases} \llbracket -\frac{N}{2}, \frac{N}{2} - 1 \rrbracket & \text{if } N \text{ even} \\ \llbracket -\frac{N-1}{2}, \frac{N-1}{2} \rrbracket & \text{if } N \text{ odd.} \end{cases} \tag{65}$$

To simplify the notation and avoid ambiguities, we use square brackets to indicate sampling, bold-face lower-case letters for vectors (indexed collections of values), and bold-face upper-case letters for linear operators (matrices). For example, $u_z(\boldsymbol{x})$ is the field in the transverse plane at longitudinal position z and lateral position $\boldsymbol{x}$, while $u_z[\boldsymbol{j}] \equiv u_z(\boldsymbol{x}[\boldsymbol{j}])$ is the sampled field at grid index $\boldsymbol{j}$. As another example, $u_z{:}\mathbb{R}^2 \to \mathbb{C}$ is the field as a continuous function of the lateral position, while $\boldsymbol{u}_z \in \mathbb{C}^{N^2}$ is the sampled field, that is the vector whose entries are $u_z[\boldsymbol{j}]$ for all $\boldsymbol{j} \in \mathbb{J}^2$.

The **sampled angular spectrum** at frequency $\boldsymbol{\alpha}[\boldsymbol{j}] = \delta\alpha \times \boldsymbol{j}$ can be computed by using a Riemman sum approximation of the continuous Fourier transform integral:

$$\begin{aligned} \widetilde{u}_z[\boldsymbol{j}] = \widetilde{u}_z(\boldsymbol{\alpha}[\boldsymbol{j}]) &= \iint \mathrm{e}^{-\mathrm{i}\,2\,\pi\,\langle \boldsymbol{\alpha}[\boldsymbol{j}], \boldsymbol{x} \rangle}\, u_z(\boldsymbol{x})\,\mathrm{d}\boldsymbol{x} \\ &\approx \delta x^2 \sum_{\boldsymbol{j}' \in \mathbb{J}^2} \underbrace{\mathrm{e}^{-\mathrm{i}\,2\,\pi\,\langle \boldsymbol{\alpha}[\boldsymbol{j}], \boldsymbol{x}[\boldsymbol{j}'] \rangle}}_{F_{\boldsymbol{j},\boldsymbol{j}'}}\, \underbrace{u_z(\boldsymbol{x}[\boldsymbol{j}'])}_{u_z[\boldsymbol{j}']} \end{aligned} \tag{66}$$

which, using linear algebra notation, yields the following numerical approximations for the sampled field and angular spectrum:

$$\widetilde{\boldsymbol{u}}_z = \delta x^2\, \mathbf{F} \cdot \boldsymbol{u}_z \tag{67}$$

$$\boldsymbol{u}_z = \delta\alpha^2\, \mathbf{F}^\star \cdot \widetilde{\boldsymbol{u}}_z \tag{68}$$

where $\mathbf{F}$ is the *discrete Fourier transform* (DFT) operator whose entries are given by:

$$F_{\boldsymbol{j},\boldsymbol{j}'} = \mathrm{e}^{-\mathrm{i}\,2\,\pi\,\langle \boldsymbol{\alpha}_{\boldsymbol{j}}, \boldsymbol{x}_{\boldsymbol{j}'} \rangle} = \mathrm{e}^{-\mathrm{i}\,2\,\pi\,\delta x\,\delta\alpha\,\langle \boldsymbol{j}, \boldsymbol{j}' \rangle} \tag{69}$$

The $N \times N$ DFT can be computed by the *fast Fourier transform* (FFT) in $\mathcal{O}(N^2\, \log_2 N)$ operations. As shown by Eqs. (156) and (160) in Appendix B, having $\mathbf{F}$ inversible imposes:

$$\delta x\, \delta\alpha = \tfrac{1}{N} \tag{70}$$

and thus:

$$F_{\boldsymbol{j},\boldsymbol{j}'} = \mathrm{e}^{-\mathrm{i}\,2\,\pi\,\langle \boldsymbol{j}, \boldsymbol{j}' \rangle / N}, \tag{71}$$

and:

$$\big(\delta x^2\, \mathbf{F}\big) \cdot \big(\delta\alpha^2\, \mathbf{F}^\star\big) = \tfrac{1}{N^2}\, \mathbf{F} \cdot \mathbf{F}^\star = \mathbf{Id}. \tag{72}$$

2.2 Propagation by convolution

As stated by Eq. (18), propagation of the field $u_0(\boldsymbol{x})$ in the input transverse plane at $z = 0$ to the transverse plane at z can be expressed as a convolution:

$$u_z(\boldsymbol{x}) = \iint h_z(\boldsymbol{x} - \boldsymbol{x}')\, u_0(\boldsymbol{x}')\, \mathrm{d}\boldsymbol{x}' \tag{73}$$

with $h_z(\boldsymbol{x})$ the propagation kernel. For the Rayleigh-Sommerfeld diffraction integral, in Eq. (38), the propagation kernel is given in Eq. (39). For Fresnel diffraction, that is in paraxial conditions, the propagation kernel is given in Eq. (44).

This type of propagation can be numerically approximated by a discrete convolution:

$$u_z[\boldsymbol{j}] = u_z(\boldsymbol{x}[\boldsymbol{j}]) \approx \sum_{\boldsymbol{j}'} h_z[\boldsymbol{j} - \boldsymbol{j}']\, u_0[\boldsymbol{j}']\, \delta x^2 \tag{74}$$

where $h_z[\boldsymbol{j} - \boldsymbol{j}'] = h_z(\delta x\, (\boldsymbol{j} - \boldsymbol{j}')) = h_z(\boldsymbol{x}[\boldsymbol{j}] - \boldsymbol{x}[\boldsymbol{j}'])$ and $u_0[\boldsymbol{j}] = u_0(\boldsymbol{x}[\boldsymbol{j}'])$ are the sampled propagation kernel and input field. The discrete convolution can be quickly computed by 3 FFTs. Give the expression in algebra notation.

There are however 2 issues to take care of:

1. To avoid aliasing, the size of the sampled area must be sufficiently large (using zero padding to extend the supports of the beam in the input and output transverse planes).

2. To provide a good approximation, the variations of all the functions involved in the convolution (the input field and the kernel) must be correctly sampled which imposes a lower bound on the sampling step δx or an upper bound of the propagation range z.

These issues are discussed next.

2.2.1 Support constraint in propagation by convolution

To limit the number of operations, the sum in the discrete convolution in Eq. (74) shall only be performed for $\boldsymbol{j}' \in \Omega_0$ where Ω_0 includes the nodes for which the field u_0 in the input transverse plane is non-zero, in other words:

$$u_0[\boldsymbol{j}'] \neq 0 \quad \Longrightarrow \quad \boldsymbol{j}' \in \Omega_0. \tag{75}$$

The discrete convolution shall also only be computed for nodes $\boldsymbol{j}$ where the field in the output transverse plane is non-zero. Due to diffraction, it is not possible to strictly impose such a restriction but we may assume that a mask is placed in the output transverse plane so that we can define Ω_z which includes the nodes where the field in the output transverse plane is non-zero *after* the mask. Said otherwise, we assume that we are only interested in having the field in the output transverse plane for a limited support Ω_z. For practical reasons and since we are interested in making as few operations as possible, the supports Ω_0 and Ω_z must be finite and shall be as small as possible.

For a faster computation of the discrete convolution, the discrete Fourier transform (DFT) may be used, but to avoid aliasing, the size of the grid must be large enough. Denoting L_0 and L_z the maximum number of samples along any dimension of Ω_0 and Ω_z, the minimal size of the support of the propagation kernel is $L = L_0 + L_z - 1$ to account for all possible values of $\boldsymbol{j} - \boldsymbol{j}'$ and the minimal output discrete convolution has size $L + L_0 - 1$. Finally, the minimal grid size is:

$$N \geq 2\,L_0 + L_z - 2. \tag{76}$$

If the supports, Ω_0, Ω_z, and $\Omega = \Omega_z - \Omega_0$ are not centered, the output angular spectrum may be multiplied by a linear phase factor before applying the inverse DFT. (Not clear and supports are assumed centered in the 2 next subsections.)

In the considered conditions and assuming square supports to simplify, the direct computation of the discrete convolution by Eq. (74) takes about $2\,L_0^2\,L_z^2 \sim 2\,L^4$ operations with L the typical value of L_0 and L_z. Computation by fast Fourier transform (FFT) takes about $3\,N^2\,\log_2 N^2 \sim 3\,(3\,L)^2\,\log_2((3\,L)^2) \sim 54\,L^2\,\log_2 L$ operations. For large[7] L's, the FFT-based method is much faster despite the larger size of the required grid.

2.2.2 Sampling and range constraints in Rayleigh-Sommerfeld diffraction

The propagation kernel $h_z(\boldsymbol{x})$ in Rayleigh-Sommerfeld diffraction is given by Eq. (39) and the most constraining term for the sampling step is the phase of the $\mathrm{e}^{\mathrm{i}\,k\,r}$ term since it varies by more than π radians when the variation of r between adjacent samples is greater than $\lambda/2$.

On a lateral grid sampled at positions $\boldsymbol{x}[\boldsymbol{j}] = \boldsymbol{j} \times \delta x$ with $\boldsymbol{j} \in \mathbb{J}^2$, the propagation distance is given by:

$$r[\boldsymbol{j}] = \sqrt{\|\boldsymbol{x}[\boldsymbol{j}]\|^2 + z^2} = \sqrt{\delta x^2\,\|\boldsymbol{j}\|^2 + z^2} \tag{77}$$

with $z > 0$ the distance along the z-axis between the input and output planes. To avoid irreversible phase wrapping, the phase difference between two adjacent nodes of the sampling grid must not be greater than π which yields the condition $k\,\delta r_{\max} \leq \pi$ or equivalently $\delta r_{\max} \leq \lambda/2$ with $\delta r_{\max}$ the greatest absolute variation of r between 2 adjacent nodes in the sampling grid:

$$\delta r_{\max} = \max_{\substack{\boldsymbol{j} \in \Omega \\ \delta\boldsymbol{j} \in \delta\Omega}} |r[\boldsymbol{j} + \delta\boldsymbol{j}] - r[\boldsymbol{j}]| \tag{78}$$

with Ω the discrete kernel support accounting for all differences in lateral positions between the input and output transverse planes and:

$$\delta\Omega = \{(\pm 1, 0), (0, \pm 1)\} \tag{79}$$

the offsets to the closest sampled nodes (the blue dots in Fig. 1).

[7] not so large in fact, since the FFT-based method is faster for $L \geq 10$ ignoring overheads

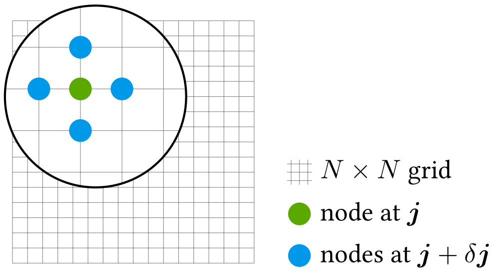

Figure 1: Closest nodes on a grid.

Since it is required that δx be small enough to correctly sample the variations of r, the following approximation can be made:

$$r[\boldsymbol{j} + \delta\boldsymbol{j}] - r[\boldsymbol{j}] \approx \left\langle \frac{\partial r[\boldsymbol{j}]}{\partial \boldsymbol{j}}, \delta\boldsymbol{j} \right\rangle = \frac{\delta x^2 \langle \boldsymbol{j}, \delta\boldsymbol{j} \rangle}{r[\boldsymbol{j}]} \tag{80}$$

where $\langle , \rangle$ denotes the inner (scalar) product. Hence:

$$\delta r_{\max} \approx \delta x^2 \max_{\substack{\boldsymbol{j} \in \Omega \\ \delta\boldsymbol{j} \in \delta\Omega}} \left| \frac{\langle \boldsymbol{j}, \delta\boldsymbol{j} \rangle}{r[\boldsymbol{j}]} \right| = \delta x^2 \max_{\boldsymbol{j} \in \Omega} \frac{\max_{\delta\boldsymbol{j} \in \delta\Omega} |\langle \boldsymbol{j}, \delta\boldsymbol{j} \rangle|}{r[\boldsymbol{j}]} \tag{81}$$

$$= \delta x^2 \max_{\boldsymbol{j} \in \Omega} \frac{\|\boldsymbol{j}\|_\infty}{r[\boldsymbol{j}]} \tag{82}$$

with $\|\boldsymbol{j}\|_\infty = \max(|j_1|, |j_2|)$ the infinite norm of $\boldsymbol{j}$. Since $r[\boldsymbol{j}] = \sqrt{\delta x^2 \, (j_1^2 + j_2^2) + z^2}$, the nodes that have a given $\|\boldsymbol{j}\|_\infty = \ell$ and yet the least $r[\boldsymbol{j}]$ are those such that $\boldsymbol{j} = (\pm\ell, 0)$ or $\boldsymbol{j} = (0, \pm\ell)$, hence:

$$\delta r_{\max} \approx \delta x \max_{\boldsymbol{j} \in \Omega} \frac{\|\boldsymbol{j}\|_\infty}{\sqrt{\|\boldsymbol{j}\|_\infty^2 + (z/\delta x)^2}}. \tag{83}$$

Deriving the function:

$$\delta r(\ell) = \frac{\ell}{\sqrt{\ell^2 + (z/\delta x)^2}} \tag{84}$$

yields:

$$\delta r'(\ell) = \frac{(z/\delta x)^2}{(\ell^2 + (z/\delta x)^2)^{3/2}} \tag{85}$$

which is non-negative, hence $\delta r(\ell)$ is increasing with ℓ. The maximal value for δr is thus found at $\ell_{\max} = \max_{\boldsymbol{j} \in \Omega} \|\boldsymbol{j}\|_\infty = L/2$ with L the lateral size of Ω in number of samples and finally:

$$\delta r_{\max} \approx \frac{\delta x \, D/2}{\sqrt{z^2 + (D/2)^2}}. \tag{86}$$

with $D = L \, \delta x$ the lateral size of Ω in length units.

The sampling condition for the Rayleigh-Sommerfeld kernel, that is $\delta r_{\max} \leq \lambda/2$, finally writes:

$$\frac{\delta x}{\sqrt{z^2 + (D/2)^2}} \leq \lambda/D. \tag{87}$$

This condition may be expressed as an upper bound on the sampling step:

$$\delta x \leq \lambda \sqrt{(z/D)^2 + 1/4} \approx \begin{cases} \lambda/2 & \text{when } |z| \ll D \\ |z|\,\lambda/D & \text{when } |z| \gg D \end{cases} \tag{88}$$

with D the lateral size of Ω. In the near field, that is for $z \ll D$, the bound is the Shannon sampling step to correctly sample all propagating waves which have spatial frequencies up to $1/\lambda$. In the far field, that is for $z \gg D$, the bound is the propagation distance along z times the angular diffraction limit λ/D for an aperture of size D. Note that, even though the angular spectrum $\widetilde{u}_0(\boldsymbol{\alpha})$ of the field in the input transverse plane has a cutoff frequency much smaller than $1/\lambda$, the maximal sampling step of $\lambda/2$ still applies to avoid phase errors in the sampled kernel before computing its discrete Fourier transform. To benefit from a cutoff frequency of the angular spectrum, another method must be considered where it is the propagation transfer function $\widetilde{h}_z(\boldsymbol{\alpha})$ which is sampled.

Looking at Eq. (88), it is clear that having the smallest possible D is desirable to relax the constraint on the smallness of the sampling step. Going back to the discussion about the sizes of the supports, near Eq. (76), it can be seen that the smallest possible support size to sample the propagation kernel is $D = D_0 + D_z$ where $D_0 = L_0\,\delta x$ and $D_z = L_z\,\delta x$ are the respective sizes of the supports of the field in the input and output transverse planes.

For a chosen sampling step, the sampling condition in Eq. (88) can be converted into a minimal range condition to apply this propagation method:

$$|z| \geq D \sqrt{(\delta x/\lambda)^2 - 1/4} \tag{89}$$

provided $\delta x > \lambda/2$ otherwise, $|z|$ can be as small as a few wavelengths[8]. Again, to relax as much as possible this constraint, D must be as small as possible.

Remember that Rayleigh-Sommerfeld diffraction integral assumes $z \geq 0$, that is forward propagation, **reverse propagation** can nevertheless be implemented as the deconvolution by the forward propagation kernel.

2.2.3 Sampling and range constraints for paraxial propagation kernel

The paraxial (Fresnel) propagation kernel is given by Eq. (44) which we recall for convenience:

$$h_z(\boldsymbol{x}) = \frac{\mathrm{e}^{\mathrm{i}\,k\,z}}{\mathrm{i}\,\lambda\,z}\,\mathrm{e}^{\mathrm{i}\,\pi\,\|\boldsymbol{x}\|^2/(\lambda\,z)}. \tag{90}$$

Now the phase is varying as $\phi(\boldsymbol{x}) = \pi\,\|\boldsymbol{x}\|^2/(\lambda\,z)$ a quadratic function of the transverse position $\boldsymbol{x}$. The maximal absolute difference of the quadratic phase between

[8] if $|z|$ is less than a few λ, evanescent waves must be taken into account

adjacent nodes of the grid is:

$$\delta\phi_{\max} = \max_{\substack{\boldsymbol{j}\in\Omega \\ \delta\boldsymbol{j}\in\delta\Omega}} |\phi(\boldsymbol{x}[\boldsymbol{j}+\delta\boldsymbol{j}]) - \phi(\boldsymbol{x}[\boldsymbol{j}])| \tag{91}$$

$$= \frac{\pi\,\delta x^2}{\lambda\,|z|} \max_{\substack{\boldsymbol{j}\in\Omega \\ \delta\boldsymbol{j}\in\delta\Omega}} \left| \|\boldsymbol{j}+\delta\boldsymbol{j}\|^2 - \|\boldsymbol{j}\|^2 \right| \tag{92}$$

with, as in the previous subsection, $\Omega = \Omega_0 - \Omega_z$ the set of nodes for which the kernel must be evaluated and $\delta\Omega$ given in Eq. (79) the offsets to the adjacent nodes. To estimate $\delta\phi_{\max}$, we compute:

$$\max_{\substack{\boldsymbol{j}\in\Omega \\ \delta\boldsymbol{j}\in\delta\Omega}} \left| \|\boldsymbol{j}+\delta\boldsymbol{j}\|^2 - \|\boldsymbol{j}\|^2 \right| = \max_{\substack{\boldsymbol{j}\in\Omega \\ \delta\boldsymbol{j}\in\delta\Omega}} \left| \|\delta\boldsymbol{j}\|^2 + 2\,\langle \boldsymbol{j}, \delta\boldsymbol{j}\rangle \right| \tag{93}$$

$$= \max_{\substack{\boldsymbol{j}\in\Omega \\ \delta\boldsymbol{j}\in\delta\Omega}} |1 + 2\,\langle \boldsymbol{j}, \delta\boldsymbol{j}\rangle| \tag{94}$$

$$= 1 + 2 \max_{\substack{\boldsymbol{j}\in\Omega \\ \delta\boldsymbol{j}\in\delta\Omega}} |\langle \boldsymbol{j}, \delta\boldsymbol{j}\rangle| \tag{95}$$

$$= 1 + 2 \max_{\boldsymbol{j}\in\Omega} \|\boldsymbol{j}\|_\infty \tag{96}$$

$$= 1 + L \tag{97}$$

where right-hand side (94) follows from $\|\delta\boldsymbol{j}\| = 1$ for any $\delta\boldsymbol{j} \in \delta\Omega$, right-hand side (96) follows from $\max_{\delta\boldsymbol{j}\in\delta\Omega} |\langle \boldsymbol{j}, \delta\boldsymbol{j}\rangle| = \|\boldsymbol{j}\|_\infty$ already proven before, and right-hand side (97) follows from $\max_{\boldsymbol{j}\in\Omega} \|\boldsymbol{j}\|_\infty = L/2$ also proven before with L the lateral size of Ω in number of samples. Note that, contrarily to the computations in Eq. (80), there are no approximations here. The maximal absolute difference of the quadratic phase

$$\delta\phi_{\max} = \max_{\substack{\boldsymbol{j}\in\Omega \\ \delta\boldsymbol{j}\in\delta\Omega}} |\phi(\boldsymbol{x}[\boldsymbol{j}+\delta\boldsymbol{j}]) - \phi(\boldsymbol{x}[\boldsymbol{j}])| = \frac{\pi\,(L+1)\,\delta x^2}{\lambda\,|z|} \approx \frac{\pi\,L\,\delta x^2}{\lambda\,|z|} \tag{98}$$

the latter approximation since $L \gg 1$ in general. Using $D = L\,\delta x = D_0 + D_z$, the lateral size of Ω in units of length, the condition $\delta\phi_{\max} \leq \pi$ amounts to:

$$\frac{D\,\delta x}{\lambda\,|z|} \leq 1 \tag{99}$$

which may be seen as an upper bound for the sampling step:

$$\delta x \leq |z|\,\lambda/D, \tag{100}$$

or as a minimal propagation range condition:

$$|z| \geq D\,\delta x/\lambda. \tag{101}$$

Compared to Eq. (88), Eq. (100) corresponds to the far field case $|z| \gg D$. Compared to Eq. (89), Eq. (101) corresponds to $\delta x \gg \lambda/2$.

Note that the paraxial condition approximation

2.3 Angular spectrum propagation

The angular spectrum propagation method is similar to the propagation by convolution computed by means of FFT's, the only difference is that the propagation transfer function is directly sampled instead of being given by a DFT of the sampled propagation kernel.

2.3.1 Propagation by the non-paraxial transfer function

Propagation of the angular spectrum:

$$\widetilde{u}_{z+\Delta z}(\boldsymbol{\alpha}) = \widetilde{h}_{\Delta z}(\boldsymbol{\alpha})\,\widetilde{u}_z(\boldsymbol{\alpha}) \quad \text{with} \quad \widetilde{h}_{\Delta z}(\boldsymbol{\alpha}) = \mathrm{e}^{\mathrm{i}\,k\,\Delta z\,\sqrt{1-\|\lambda\,\boldsymbol{\alpha}\|^2}}$$

is numerically approximated by:

$$\begin{aligned} \boldsymbol{u}_{z+\Delta z} &= \big(\delta\alpha^2\,\mathbf{F}^\star\big)\cdot\mathrm{diag}\big(\mathrm{e}^{\mathrm{i}\,\phi}\big)\cdot\big(\delta x^2\,\mathbf{F}\big)\cdot\boldsymbol{u}_z \\ &= \underbrace{\frac{1}{N^2}\cdot\mathbf{F}^\star\cdot\mathrm{diag}\big(\mathrm{e}^{\mathrm{i}\,\phi}\big)\cdot\mathbf{F}}_{\text{propagator}}\cdot\boldsymbol{u}_z \end{aligned} \tag{102}$$

since $\delta x\,\delta\alpha = 1/N$ for the approximation of the Fourier transform by the DFT operator $\mathbf{F}$ and with a frequency-wise phase shift ϕ given by:

$$\phi[\boldsymbol{j}] = k\,\Delta z\,\sqrt{1-\|\lambda\,\boldsymbol{\alpha}_{\boldsymbol{j}}\|^2} = k\,\Delta z\,\sqrt{1-\|\varepsilon\,\boldsymbol{j}\|^2} \tag{103}$$

with $\varepsilon = \lambda\,\delta\alpha = \lambda/(N\,\delta x)$, usually $\varepsilon \ll 1$.

2.3.2 Short range limit of the angular spectrum

For the DFT to be a good approximation of the continuous Fourier transform, the sampled functions must vary slowly between consecutive samples. In particular for the phase shift:

$$|\phi[\boldsymbol{j}+\delta\boldsymbol{j}] - \phi[\boldsymbol{j}]| \le \pi \tag{104}$$

must hold $\forall\boldsymbol{j}\in\Omega$ and $\forall\delta\boldsymbol{j}\in\delta\Omega$ with:

$$\Omega = \big\{\boldsymbol{j}\in\mathbb{J}^2 \;\big|\; \|\boldsymbol{j}\| < \alpha_{\max}/\delta\alpha\big\} \tag{105}$$

the domain where spatial frequencies are below the cutoff frequency $\alpha_{\max}$ of the angular spectrum $\widetilde{u}_z$ and:

$$\delta\Omega = \{(\pm 1, 0), (0, \pm 1)\} \tag{106}$$

the offsets to the closest spatial frequencies (see blue dots in the figure).

Note that $\alpha_{\max}$ may be infinite. We introduce:

$$\alpha_{\text{Nyquist}} = \frac{1}{2}\,N\,\delta\alpha = \frac{1}{2\,\delta x} \tag{107}$$

the Nyquist frequency.

This imposes a short range limit: $\boxed{|\Delta z| \le \frac{N\,\delta x^2}{\lambda}\,\sqrt{1-\tfrac{1}{2}\,(N\,\varepsilon)^2}}$

2.3.3 Short range limit of the angular spectrum (demonstration)

The constraint in Eq. (104) that must hold for any $\forall \boldsymbol{j} \in \Omega$ and $\forall \delta\boldsymbol{j} \in \delta\Omega$ equivalently holds for the maximal absolute value of the sampled phase difference:

$$\begin{aligned} & |\phi[\boldsymbol{j}+\delta\boldsymbol{j}] - \phi[\boldsymbol{j}]| \leq \pi \quad \forall \boldsymbol{j} \in \Omega,\ \forall \delta\boldsymbol{j} \in \delta\Omega \\ \iff \quad & \max_{\substack{\boldsymbol{j}\in\Omega \\ \delta\boldsymbol{j}\in\delta\Omega}} |\phi[\boldsymbol{j}+\delta\boldsymbol{j}] - \phi[\boldsymbol{j}]| \leq \pi \end{aligned} \tag{108}$$

The maximal value can be estimated as follows:

$$\max_{\substack{\boldsymbol{j}\in\Omega \\ \delta\boldsymbol{j}\in\delta\Omega}} |\phi[\boldsymbol{j}+\delta\boldsymbol{j}] - \phi[\boldsymbol{j}]| \simeq \max_{\substack{\boldsymbol{j}\in\Omega \\ \delta\boldsymbol{j}\in\delta\Omega}} \left| \left\langle \frac{\partial \phi[\boldsymbol{j}]}{\partial \boldsymbol{j}}, \delta\boldsymbol{j} \right\rangle \right| \tag{109}$$

$$= k\,|\Delta z|\,\varepsilon^2 \max_{\substack{\boldsymbol{j}\in\Omega \\ \delta\boldsymbol{j}\in\delta\Omega}} \left| \frac{\langle \boldsymbol{j}, \delta\boldsymbol{j}\rangle}{\sqrt{1-\|\varepsilon\,\boldsymbol{j}\|^2}} \right| \tag{110}$$

since $\phi[\boldsymbol{j}] = k\,\Delta z\,\sqrt{1-\|\varepsilon\,\boldsymbol{j}\|^2}$. Then

$$\max_{\substack{\boldsymbol{j}\in\Omega \\ \delta\boldsymbol{j}\in\delta\Omega}} \left| \frac{\langle \boldsymbol{j}, \delta\boldsymbol{j}\rangle}{\sqrt{1-\|\varepsilon\,\boldsymbol{j}\|^2}} \right| = \max_{\boldsymbol{j}\in\Omega} \frac{\max_{\delta\boldsymbol{j}\in\delta\Omega} |\langle \boldsymbol{j}, \delta\boldsymbol{j}\rangle|}{\left|\sqrt{1-\|\varepsilon\,\boldsymbol{j}\|^2}\right|} = \max_{\boldsymbol{j}\in\Omega} \frac{\|\boldsymbol{j}\|_\infty}{\left|\sqrt{1-\|\varepsilon\,\boldsymbol{j}\|^2}\right|} \tag{111}$$

$$\tag{112}$$

with $\|\boldsymbol{j}\|_\infty = \max(|j_1|, |j_2|)$ the infinite norm of $\boldsymbol{j}$. Introducing $L = \max_{\boldsymbol{j}\in\Omega}\|\boldsymbol{j}\| \leq N/\sqrt{2}$ and noting that $L \leq N/\sqrt{2}$ due to the finite number of samples along a lateral dimension, there are 2 cases to consider:

- If $\max_{\boldsymbol{j}\in\Omega}\|\boldsymbol{j}\| \geq 1/\varepsilon$, then the sampled spatial frequencies include evanescent waves and $\sqrt{1-\|\varepsilon\,\boldsymbol{j}\|^2}$ may be arbitrarily close to zero for $\|\boldsymbol{j}\|_\infty > 0$. Hence, the condition in Eq. (104) cannot hold and aliasing is unavoidable.

- If $\varepsilon\,L < 1$, then the sampled spatial frequencies include evanescent waves and $\sqrt{1-\|\varepsilon\,\boldsymbol{j}\|^2}$ may be arbitrarily small. If $N/2 \leq L \leq N/\sqrt{2}$, then any point on the circle defined by $\|\boldsymbol{j}\|_2 = L$ yields the minimal value of the denominator and the maximal value of the numerator. If $L \leq N/2$, then any point at the intersection of the square and of the circle defined by $\|\boldsymbol{j}\|_2 = L$ yields the minimal value of the denominator and the maximal value of the numerator. Hence: Figure 2 shows the different possibilities in that case. Form that figure, it can be deduced that

$$\max_{\boldsymbol{j}\in\Omega} \frac{\|\boldsymbol{j}\|_\infty}{\left|\sqrt{1-\|\varepsilon\,\boldsymbol{j}\|^2}\right|} \approx \frac{\min(L, N/2)}{\sqrt{1-(\varepsilon\,L)^2}} \tag{113}$$

and, since the numerator of the above right-hand side is nearly a non-decreasing function of $\|\boldsymbol{j}\|$ while the denominator is a non-increasing function of $\|\boldsymbol{j}\|$,

$$\max_{\boldsymbol{j}\in\Omega} \frac{\|\boldsymbol{\alpha}_{\boldsymbol{j}}\|_\infty}{\left|\sqrt{1-\|\lambda\,\boldsymbol{\alpha}_{\boldsymbol{j}}\|^2}\right|} \approx \frac{\min(L, N/2)}{\sqrt{1-(\varepsilon\,L)^2}} \tag{114}$$

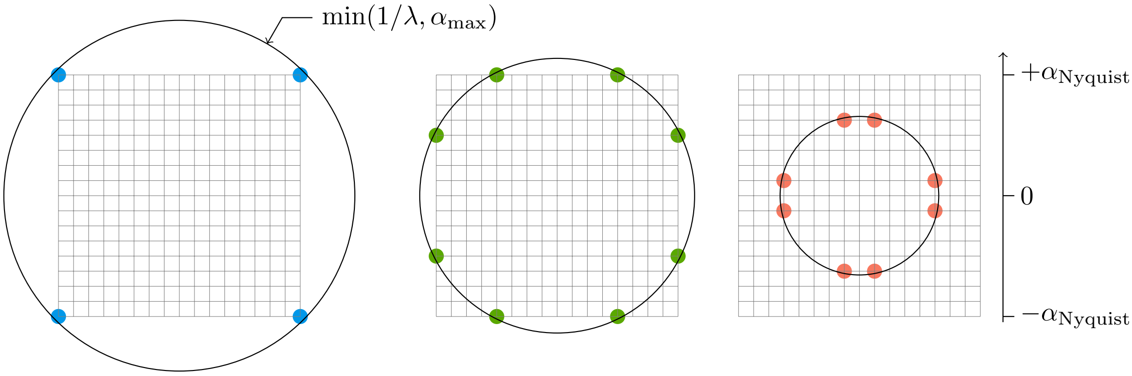

Figure 2: Discrete spatial frequencies (indicated by colored circles) where the phase wrapping is the most severe for the non-paraxial propagation transfer function. The $N \times N$ grid indicates the positions of the discrete frequencies. The circle indicates the smallest of the cutoff frequency of the angular spectrum and of the evanescent waves limit at $1/\lambda$ for the 3 possible cases.

We have shown that:

$$\max_{\substack{\boldsymbol{j}\in\Omega \\ \delta\boldsymbol{j}\in\delta\Omega}} |\phi[\boldsymbol{j}+\delta\boldsymbol{j}] - \phi[\boldsymbol{j}]| \simeq k\,|\Delta z|\,\varepsilon^2 \frac{\min(L, N/2)}{\sqrt{1-(\varepsilon\,L)^2}} \quad \text{with } L = \max_{\boldsymbol{j}\in\Omega} \|\boldsymbol{j}\| \leq N/\sqrt{2}$$

Hence:

$$|\phi[\boldsymbol{j}+\delta\boldsymbol{j}] - \phi[\boldsymbol{j}]| \leq \pi \quad \forall \boldsymbol{j}\in\Omega,\ \forall \delta\boldsymbol{j}\in\delta\Omega$$

amounts to:

$$\begin{aligned} |\Delta z| \leq \frac{\pi\,\sqrt{1-(\varepsilon\,L)^2}}{k\,\varepsilon^2\,\min(L, N/2)} &= \frac{\lambda\,\sqrt{1-(\varepsilon\,L)^2}}{2\,\varepsilon^2\,\min(L, N/2)} && \text{since } k = 2\,\pi/\lambda \\ &= \frac{N^2\,\delta x^2\,\sqrt{1-(\varepsilon\,L)^2}}{2\,\lambda\,\min(L, N/2)} && \text{since } \varepsilon = \lambda\,\delta\alpha = \frac{\lambda}{N\,\delta x} \end{aligned}$$

2 possibilities:

- If $L = \max_{\boldsymbol{j}\in\Omega}\|\boldsymbol{j}\| < N/\sqrt{2}$, then the limit is $|\Delta z| \leq 0$.
- If $L = \max_{\boldsymbol{j}\in\Omega}\|\boldsymbol{j}\| = N/\sqrt{2}$, then the limit is $|\Delta z| \leq \dfrac{N\,\delta x^2}{\lambda}\,\sqrt{1-\frac{1}{2}\,(\varepsilon\,N)^2}$. (Q.E.D.)

2.4 Discrete computations

See **?** and **?**.

Several methods have been proposed for the numerical propagation of two-dimensional sampled planar fields of size $N \times N$. Discrete approximation by a Riemann sum of the diffraction integral equation requires $\mathcal{O}(N^4)$ numerical floating-point operations, finite difference methods to numerically solve the differential Helmholtz equation is as demanding because of the number of steps to propagate the wave (?). Using the Fast Fourier Transform (FFT) to compute the convolution product (the so-called angular spectrum method) requires $\mathcal{O}(N^2 \log_2 N)$ operations but imposes that the sampling steps δx in the transverse planes be the same along the propagation.

Angular spectrum propagation. In this method, the propagation between a transverse plane at z_0 to a transverse plane at $z_1 = z_0 + \Delta z$ is implemented by a discrete convolution of the field u_{z_0} by the shift-invariant propagation kernel $h_{\Delta z}$. For speed, the discrete convolution is computed by means of Fast Fourier Transforms (FFTs).

The sampled angular spectrum is given by:

$$\begin{aligned}
\widetilde{\boldsymbol{u}}_z[\ell_1,\ell_2] &= \widetilde{u}_z(\alpha[\ell_1],\beta[\ell_2]) \\
&= \iint u_z(x,y)\,\mathrm{e}^{-\mathrm{i}\,2\,\pi\,(\alpha[\ell_1]\,x,\beta[\ell_2]\,y)}\mathrm{d}x\,\mathrm{d}y \\
&\approx \sum_{k_1,k_2} u_z(x[j_1],y[j_2])\,\mathrm{e}^{-\mathrm{i}\,2\,\pi\,(\alpha[\ell_1]\,x[j_1],\beta[\ell_2]\,y[j_2])}\,|\delta x\,\delta y| \\
&= |\delta x\,\delta y|\,\big(\mathbf{F}\cdot\boldsymbol{u}_z\big)[\ell_1,\ell_2] \qquad (115)
\end{aligned}$$

where $\mathbf{F}$ is the forward DFT operator (see Appendix **??**), $\boldsymbol{u}_z$ is the sampled field $u_z(x,y)$ with sampling step sizes δx and δy along the x and y dimensions, and the square brackets are used to index the sampled quantities (as in the first line of the above equation). According to the properties of the DFT, the discrete angular spectrum $\widetilde{\boldsymbol{u}}_z$ is sampled with steps $\delta\alpha = 1/(N_1\,\delta x)$ and $\delta\beta = 1/(N_2\,\delta y)$. In the following, we assume that the sampling steps and the number of samples are the same along the two transverse Cartesian axes so that: $N_1 = N_2 = N$ and $\delta x = \delta y$ and thus:

$$\widetilde{\boldsymbol{u}}_z = |\delta x|^2\,\mathbf{F}\cdot\boldsymbol{u}_z, \qquad (116)$$

is the discrete angular spectrum with frequency sampling steps $\delta\alpha = \delta\beta = 1/(N\,\delta x)$. Conversely:

$$\boldsymbol{u}_z = |\delta\alpha|^2\,\mathbf{F}^\star\cdot\widetilde{\boldsymbol{u}}_z, \qquad (117)$$

where $\mathbf{F}^\star$, the adjoint of $\mathbf{F}$, is the backward DFT operator. It is easy to check that Eq. (117) with $\delta\alpha = 1/(N\,\delta x)$ is indeed the inverse of Eq. (116):

$$|\delta\alpha|^2\,\mathbf{F}^\star\cdot\widetilde{\boldsymbol{u}}_z = \frac{1}{(N\,|\delta x|)^2}\,\mathbf{F}^\star\cdot\big(|\delta x|^2\,\mathbf{F}\cdot\boldsymbol{u}_z\big) = \frac{1}{N^2}\,\mathbf{F}^\star\cdot\mathbf{F}\cdot\boldsymbol{u}_z = \boldsymbol{u}_z$$

where the last simplification follows from Eq. (**??**). The field in the transverse plane at z_1 knowing the field in the transverse plane at z_0 is given by:

$$\boldsymbol{u}_{z_1} = \frac{1}{N^2}\,\mathbf{F}^\star\cdot\mathrm{diag}\big(\widetilde{\boldsymbol{h}}_{z_1-z_0}\big)\cdot\mathbf{F}\cdot\boldsymbol{u}_{z_0} \qquad (118)$$

where $\mathrm{diag}(\boldsymbol{a})$ denotes a diagonal linear operator whose diagonal entries are those of $\boldsymbol{a}$ and such that applying this operator to, say, $\boldsymbol{b}$ yields the element-wise multiplication of $\boldsymbol{a}$ and $\boldsymbol{b}$. In the above equation, $\widetilde{\boldsymbol{h}}_{z_1-z_0}$ is either the discrete Fourier transform, as defined in Eq. (116), of the propagation kernel $h_{z_1-z_0}(x,y)$ sampled with steps of size δx or $\widetilde{h}_{z_1-z_0}(\boldsymbol{\alpha})$ sampled with steps of size $\delta\alpha = 1/(N\,\delta x)$. Due to the approximation of the continuous Fourier transform by the discrete transform, the two are not exactly equivalent.

The operator implementing the propagation by means of the angular spectrum writes:

$$\mathbf{H}_z^{\text{conv}} = \frac{1}{N^2}\,\mathbf{F}^\star \cdot \operatorname{diag}\big(\widetilde{\boldsymbol{h}}_z\big) \cdot \mathbf{F}. \tag{119}$$

With this method, the sampling steps are unchanged and the exact or paraxial planar propagation may be modeled. The methods considered next specifically implement Fresnel diffraction that is assuming the paraxial approximation.

To avoid aliasing, $\mathcal{D}_{1/\lambda}$ must be inside the support sampled by the discrete frequencies. Hence, the Nyquist frequency must not be smaller than $1/\lambda$ which writes:

$$(N/2)\,\delta\alpha \geq 1/\lambda \quad\iff\quad \delta x \leq \lambda/2. \tag{120}$$

Single-FFT Fresnel propagation. In the paraxial approximation (Fresnel diffraction), the propagation kernel is given by Eq. (44) and the resulting field in transverse plane at $z_1 = z_0 + \Delta z$ is:

$$\begin{aligned} u_{z_1}(\boldsymbol{x}_1) &= \iint u_{z_0}(\boldsymbol{x}_0)\,h_{\Delta z}(\boldsymbol{x}_1 - \boldsymbol{x}_0)\,\mathrm{d}\boldsymbol{x}_0 \\ &= \frac{\mathrm{e}^{\mathrm{i}\,k\,\Delta z}}{\mathrm{i}\,\lambda\,\Delta z} \iint u_{z_0}(\boldsymbol{x}_0)\,\mathrm{e}^{\mathrm{i}\,k\,\frac{\|\boldsymbol{x}_1-\boldsymbol{x}_0\|^2}{2\,\Delta z}}\,\mathrm{d}\boldsymbol{x}_0 \\ &= \frac{\mathrm{e}^{\mathrm{i}\,k\,\Delta z}}{\mathrm{i}\,\lambda\,\Delta z}\,\mathrm{e}^{\mathrm{i}\,k\,\frac{\|\boldsymbol{x}_1\|^2}{2\,\Delta z}} \iint \Big[u_{z_0}(\boldsymbol{x}_0)\,\mathrm{e}^{\mathrm{i}\,k\,\frac{\|\boldsymbol{x}_0\|^2}{2\,\Delta z}}\Big]\,\mathrm{e}^{-\mathrm{i}\,k\,\frac{\langle\boldsymbol{x}_1,\boldsymbol{x}_0\rangle}{\Delta z}}\,\mathrm{d}\boldsymbol{x}_0 \end{aligned} \tag{121}$$

where the integral in the last right-hand side is similar to taking the Fourier transform of the term in square brackets. This integral can thus be computed by a single DFT provided the sampling condition in Eq. (160) holds which imposes that:

$$\frac{k\,\delta x_0\,\delta x_1}{\Delta z} = \pm\frac{2\,\pi}{N} \tag{122}$$

with N the number of samples along a lateral dimension. The sampling step in the output plane is thus given by:

$$\delta x_1 = \frac{\lambda\,|\Delta z|}{N\,\delta x_0} \tag{123}$$

and the double integral is approximated by $\delta x_0^2\,\mathbf{F}$ if $\Delta z > 0$ and by $\delta x_0^2\,\mathbf{F}^\star$ if $\Delta z < 0$ with $\mathbf{F}$ the two-dimensional discrete Fourier transform operator (see Appendix B). Note that, with this latter convention, the lateral axes (x and y) keep their orientation.

Using bold lowercase symbols to represent sampled quantities and bold uppercase symbols to represent operators, **single-FFT Fresnel propagation** writes:

$$\boxed{\begin{aligned}
&\boldsymbol{u}_{z_1} = \frac{\delta x_0^2\,\mathrm{e}^{\mathrm{i}\,k\,\Delta z}}{\mathrm{i}\,\lambda\,\Delta z}\,\mathbf{Q}_{\frac{\delta x_1^2}{\lambda\,\Delta z}}\cdot\mathbf{F}_{\Delta z}\cdot\mathbf{Q}_{\frac{\delta x_0^2}{\lambda\,\Delta z}}\cdot\boldsymbol{u}_{z_0}\\
&\delta x_1 = \frac{\lambda\,|\Delta z|}{N\,\delta x_0}\\
&\Delta z = z_1 - z_0\\
&\mathbf{F}_{\Delta z} = \begin{cases}\mathbf{F} & \text{if } \Delta z > 0,\\ \mathbf{F}^\star & \text{if } \Delta z < 0\end{cases}\\
&\mathbf{Q}_\rho = \mathrm{diag}(\boldsymbol{q}_\rho) \quad \text{with} \quad \boldsymbol{q}_\rho[\boldsymbol{j}] = \mathrm{e}^{\mathrm{i}\,\pi\,\rho\,\|\boldsymbol{j}\|^2} \quad \forall \boldsymbol{j}\in\mathbb{J}\times\mathbb{J}
\end{aligned}} \tag{124}$$

where operator $\mathbf{F}_{\Delta z}$ is to simplify the notation while operator $\mathbf{Q}_\rho$ implements element-wise multiplication by a quadratic phase factor. Note that multiplication by the scalar δx_0^2 commutes with all operators but that operators $\mathbf{F}_{\Delta z}$ and $\mathbf{Q}_\rho$ do not commute. Also note that $\boldsymbol{u}_{z_0}$ and $\boldsymbol{u}_{z_1}$ denote the complex amplitude in the transverse planes respectively at z_0 and z_1 and respectively sampled with steps δx_0 and δx_1 which are related by Eq. (123) and are usually not equal.

In continuous coordinates, the quadratic phase factors is given by:

$$\mathcal{Q}_\rho(\boldsymbol{x}) = \mathrm{e}^{\mathrm{i}\,\pi\,\rho\,\|\boldsymbol{x}\|^2}, \tag{125}$$

whose two-dimensional Fourier transform is:

$$\widetilde{\mathcal{Q}}_\rho = \frac{\mathrm{i}}{\rho}\,\mathcal{Q}_{-1/\rho}. \tag{126}$$

Two-step Fresnel propagation. To circumvent the limitations of the Fresnel method, the propagation by Δz can be split in 2 steps, by $\Delta z'$ and then by $\Delta z''$ such that $\Delta z' + \Delta z'' = \Delta z$. By Eq. (123), the sampling steps, δx_m and δx_1, after these two Fresnel propagation steps are given by:

$$\delta x_\mathrm{m} = \frac{\lambda\,|\Delta z'|}{N\,\delta x_0}, \tag{127a}$$

$$\delta x_1 = \frac{\lambda\,|\Delta z''|}{N\,\delta x_\mathrm{m}} = \left|\frac{\Delta z''}{\Delta z'}\right|\delta x_0 = |\overline{\gamma}|\,\delta x_0 \tag{127b}$$

with (the minus sign is to simplify equations to come):

$$\overline{\gamma} = \frac{-\Delta z''}{\Delta z'}. \tag{128}$$

Hence an arbitrary magnification $\gamma = |\overline{\gamma}| = \delta x_1/\delta x_0$ can be achieved by a 2-step Fresnel propagation with $\Delta z'$ and $\Delta z''$ given by:

$$\Delta z/\Delta z' = 1 - \overline{\gamma}, \tag{129a}$$

$$\Delta z/\Delta z'' = 1 - 1/\overline{\gamma}. \tag{129b}$$

Since $\overline{\gamma} = \pm\gamma$, there are 2 possible choices for a given magnification γ.

Using the operators notation, the 2-step Fresnel propagation yields the following sampled complex amplitude in the transverse plane at z_1:

$$
\begin{aligned}
\boldsymbol{u}_{z_1} &= \frac{\mathrm{e}^{\mathrm{i}\,k\,\Delta z''}}{\mathrm{i}\,\lambda\,\Delta z''}\,\mathbf{Q}_{\frac{\delta x_1^2}{\lambda\,\Delta z''}} \cdot \delta x_\mathrm{m}^2\,\mathbf{F}_{\Delta z''} \cdot \mathbf{Q}_{\frac{\delta x_\mathrm{m}^2}{\lambda\,\Delta z''}} \cdot \boldsymbol{u}_{z_\mathrm{m}} \\
&= \frac{\mathrm{e}^{\mathrm{i}\,k\,(\Delta z'+\Delta z'')}}{(\mathrm{i}\,\lambda)^2\,\Delta z'\,\Delta z''}\,\delta x_\mathrm{m}^2\,\delta x_0^2\,\mathbf{Q}_{\frac{\delta x_1^2}{\lambda\,\Delta z''}} \cdot \mathbf{F}_{\Delta z''} \cdot \mathbf{Q}_{\frac{\delta x_\mathrm{m}^2}{\lambda}\left(\frac{1}{\Delta z''}+\frac{1}{\Delta z'}\right)} \cdot \mathbf{F}_{\Delta z'} \cdot \mathbf{Q}_{\frac{\delta x_0^2}{\lambda\,\Delta z'}} \cdot \boldsymbol{u}_{z_0} \\
&= \frac{-\mathrm{e}^{\mathrm{i}\,k\,\Delta z}}{N^2}\,\frac{\Delta z'}{\Delta z''}\,\mathbf{Q}_{\frac{\delta x_1^2}{\lambda\,\Delta z''}} \cdot \mathbf{F}_{\Delta z''} \cdot \mathbf{Q}_{\frac{\delta x_\mathrm{m}^2}{\lambda}\left(\frac{1}{\Delta z''}+\frac{1}{\Delta z'}\right)} \cdot \mathbf{F}_{\Delta z'} \cdot \mathbf{Q}_{\frac{\delta x_0^2}{\lambda\,\Delta z'}} \cdot \boldsymbol{u}_{z_0} \quad (130)
\end{aligned}
$$

where $z_\mathrm{m} = z_0 + \Delta z'$ is the position of the intermediate transverse plane. Then using, Eqs. (127a), (127b), (129a) and (129b), the sampled complex amplitude obtained by the 2-step Fresnel propagation writes:

$$
\boxed{\boldsymbol{u}_{z_1} = \frac{\mathrm{e}^{\mathrm{i}\,k\,\Delta z}}{\overline{\gamma}\,N^2}\,\mathbf{Q}_{\frac{\overline{\gamma}\,(\overline{\gamma}-1)\,\delta x_0^2}{\lambda\,\Delta z}} \cdot \mathbf{F}_{\Delta z''} \cdot \mathbf{Q}_{\frac{-\lambda\,\Delta z}{\overline{\gamma}\,N^2\,\delta x_0^2}} \cdot \mathbf{F}_{\Delta z'} \cdot \mathbf{Q}_{\frac{(1-\overline{\gamma})\,\delta x_0^2}{\lambda\,\Delta z}} \cdot \boldsymbol{u}_{z_0}} \quad (131)
$$

with the same operators as defined in Eq. (124).

Note that, if the same step size is chosen, then $\gamma = 1$ and $\overline{\gamma} = \pm 1$. However, taking $\overline{\gamma} = 1$ and since $\mathbf{Q}_0 = \mathbf{I}$ the identity, the propagated complex visibility writes:

$$
\boldsymbol{u}_{z_1} = \frac{\mathrm{e}^{\mathrm{i}\,k\,\Delta z}}{N^2}\,\mathbf{F}_{\Delta z''} \cdot \mathbf{Q}_{\frac{-\lambda\,\Delta z}{N^2\,\delta x_0^2}} \cdot \mathbf{F}_{\Delta z'} \cdot \boldsymbol{u}_{z_0} \quad (132)
$$

which is the expression computed using the angular spectrum (check this, notably FFT direction).

To relax a bit anti-aliasing conditions, one should account for the limited spectral bandwidth of the angular spectrum and for the limited beam size.

To avoid aliasing in the central quadratic phase factor of Eq. (131) the following condition must hold:

$$
\left|\frac{\lambda\,\Delta z}{\overline{\gamma}\,N^2\,\delta x_0^2}\right| \le \frac{1}{N} \quad \Longleftrightarrow \quad \gamma = |\overline{\gamma}| \ge \frac{\lambda\,|\Delta z|}{N\,\delta x_0^2} \quad (133)
$$

Furthermore, assuming the wavefront of $\boldsymbol{u}_{z_0}$ has a curvature $1/R_0$, avoiding aliasing in the rightmost quadratic phase factor imposes that:

$$
\left|\frac{\delta x_0^2}{\lambda}\left(\frac{1-\overline{\gamma}}{\Delta z} + \frac{1}{R_0}\right)\right| \le \frac{1}{N} \quad \Longleftrightarrow \quad 1 + \frac{\Delta z}{R_0} - \frac{\lambda\,|\Delta z|}{N\,\delta x_0^2} \le \overline{\gamma} \le 1 + \frac{\Delta z}{R_0} + \frac{\lambda\,|\Delta z|}{N\,\delta x_0^2} \quad (134)
$$

For a plane input wavefront, *i.e.* $1/R_0 = 0$, with $\lambda = 500\,\mathrm{nm}$, $\delta x_0 = 0.1\,\mathrm{mm}$, $|\Delta z| = 10\,\mathrm{cm}$, and $N = 1024$, conditions in Eqs. (133) and (134) are $|\overline{\gamma}| \ge 48.8$ and $-47.8 \le \overline{\gamma} \le 49.8$. Combining the two yields $48.8 \le \overline{\gamma} \le 49.8$ which is quite restrictive and leads to have $\delta x_1 \in [4.88, 4.98]\,\mathrm{mm}$.

Angular spectrum propagation with magnification. In his book, **?** recalls the approach of **?** and **?** who rewrote the Fresnel propagation integral so as to be able to change the sampling rate of the result. Their idea is that, to have a sampling step δx_1 in the output transverse plane at z_1 that is different from the sampling step δx_0 in the input transverse plane at z_0, Fresnel propagation integral in Eq. (45) should be rewritten to yield $u'_{z_1}(\boldsymbol{x}'_1) = u_{z_1}(\gamma\,\boldsymbol{x}'_1)$ with $\boldsymbol{x}'_1 = \boldsymbol{x}_1/\gamma$ and $\gamma = \delta x_1/\delta x_0$ the desired magnification. Their method is detailed next.

Using the identity:

$$\|\boldsymbol{x}_1 - \boldsymbol{x}_0\|^2 = \gamma\,\|\boldsymbol{x}_1/\gamma - \boldsymbol{x}_0\|^2 + (1-\gamma)\,\|\boldsymbol{x}_0\|^2 + (1-1/\gamma)\,\|\boldsymbol{x}_1\|^2 \tag{135}$$

which holds for any $\gamma \neq 0$ as is easily proven by expanding the squares, the Fresnel propagation equation in Eq. (45) can be rewritten as:

$$\begin{aligned} u_{z_1}(\boldsymbol{x}_1) &= \frac{\mathrm{e}^{\mathrm{i}\,k\,\Delta z}}{\mathrm{i}\,\lambda\,\Delta z} \iint u_{z_0}(\boldsymbol{x}_0)\,\mathrm{e}^{\frac{\mathrm{i}\,k\,\|\boldsymbol{x}_1-\boldsymbol{x}_0\|^2}{2\,\Delta z}}\,\mathrm{d}\boldsymbol{x}_0 \\ &= \frac{\mathrm{e}^{\mathrm{i}\,k\,\Delta z}}{\mathrm{i}\,\lambda\,\Delta z}\,\mathrm{e}^{\frac{\mathrm{i}\,k\,(1-1/\gamma)\,\|\boldsymbol{x}_1\|^2}{2\,\Delta z}} \iint \left[u_{z_0}(\boldsymbol{x}_0)\,\mathrm{e}^{\frac{\mathrm{i}\,k\,(1-\gamma)\,\|\boldsymbol{x}_0\|^2}{2\,\Delta z}}\right] \mathrm{e}^{\frac{\mathrm{i}\,k\,\gamma\,\|\boldsymbol{x}_1/\gamma-\boldsymbol{x}_0\|^2}{2\,\Delta z}}\,\mathrm{d}\boldsymbol{x}_0 \end{aligned} \tag{136}$$

Then, with $\boldsymbol{x}'_1 = \boldsymbol{x}_1/\gamma$, $u'_{z_1}(\boldsymbol{x}'_1) = u_{z_1}(\gamma\,\boldsymbol{x}'_1)$ and:

$$u''_{z_0}(\boldsymbol{x}_0) = u_{z_0}(\boldsymbol{x}_0)\,\mathrm{e}^{\frac{\mathrm{i}\,k\,(1-\gamma)\,\|\boldsymbol{x}_0\|^2}{2\,\Delta z}} = u_{z_0}(\boldsymbol{x}_0)\,\mathrm{e}^{\mathrm{i}\,\pi\,\frac{(1-\gamma)\,\|\boldsymbol{x}_0\|^2}{\lambda\,\Delta z}},$$

the Fresnel propagation equation becomes:

$$u'_{z_1}(\boldsymbol{x}'_1) = \frac{\mathrm{e}^{\mathrm{i}\,k\,\Delta z}}{\mathrm{i}\,\lambda\,\Delta z}\,\mathrm{e}^{\frac{\mathrm{i}\,\pi\,\gamma\,(\gamma-1)\,\|\boldsymbol{x}'_1\|^2}{\lambda\,\Delta z}} \iint u''_{z_0}(\boldsymbol{x}_0)\,\mathrm{e}^{\frac{\mathrm{i}\,k\,\gamma\,\|\boldsymbol{x}'_1-\boldsymbol{x}_0\|^2}{2\,\Delta z}}\,\mathrm{d}\boldsymbol{x}_0 \tag{137}$$

where the integral reads as the convolution of $u''_{z_0}(\boldsymbol{x}_0)$ by the kernel:

$$h(\boldsymbol{x}) = \mathrm{e}^{\frac{\mathrm{i}\,k\,\gamma\,\|\boldsymbol{x}\|^2}{2\,\Delta z}}. \tag{138}$$

Using Eqs. (41) and (44), the Fourier transform of this kernel is:

$$\widetilde{h}(\boldsymbol{\alpha}) = \frac{\mathrm{i}\,\lambda\,\Delta z}{\gamma}\,\mathrm{e}^{-\mathrm{i}\,\pi\,\lambda\,\|\boldsymbol{\alpha}\|^2\,\Delta z/\gamma}, \tag{139}$$

which may be used to rewrite the convolution as the inverse Fourier transform of the product of $\widetilde{u}''_{z_0}(\boldsymbol{\alpha})$, the Fourier transform of $u''_{z_0}(\boldsymbol{x}_0)$, and of $\widetilde{h}(\boldsymbol{\alpha})$:

$$u'_{z_1}(\boldsymbol{x}'_1) = \frac{\mathrm{e}^{\mathrm{i}\,k\,\Delta z}}{\gamma}\,\mathrm{e}^{\frac{\mathrm{i}\,\pi\,\gamma\,(\gamma-1)\,\|\boldsymbol{x}'_1\|^2}{\lambda\,\Delta z}}\,\mathcal{F}^{-1}\Big\{\widetilde{u}''_{z_0}(\boldsymbol{\alpha})\,\mathrm{e}^{-\mathrm{i}\,\pi\,\lambda\,\|\boldsymbol{\alpha}\|^2\,\Delta z/\gamma}\,\Big|\,\boldsymbol{\alpha}\to\boldsymbol{x}'_1\Big\}. \tag{140}$$

Using discrete Fourier transforms (DFTs) and sampled complex amplitudes to approximate the above equation yields $\boldsymbol{u}'_{z_1}$, the complex amplitude $u'_{z_1}(\boldsymbol{x}'_1)$ sampled with a step $\delta x'_1 = \delta x_0$ because the convolution has been approximated by DFTs. Since $u'_{z_1}(\boldsymbol{x}'_1) = u_{z_1}(\gamma\,\boldsymbol{x}'_1)$, $\boldsymbol{u}'_{z_1}$ is also $\boldsymbol{u}_{z_1}$, the complex amplitude $u_{z_1}(\boldsymbol{x}_1)$ sampled with a step $\delta x_1 = \gamma\,\delta x'_1 = \gamma\,\delta x_0$. Hence, by rewriting Fresnel propagation with the angular spectrum (because a convolution has been used) as described above, an arbitrary magnification $\gamma = \delta x_1/\delta x_0$ can be chosen. Using the discrete operators previously introduced the complex amplitude in transverse plane at z_1 sampled with step $\delta x_1 = \gamma\,\delta x_0$ writes:

$$\boxed{\boldsymbol{u}_{z_1} = \frac{\mathrm{e}^{\mathrm{i}\,k\,\Delta z}}{\gamma\,N^2}\,\mathbf{Q}_{\frac{\gamma\,(\gamma-1)\,\delta x_0^2}{\lambda\,\Delta z}}\cdot\mathbf{F}^{\star}\cdot\mathbf{Q}_{\frac{-\lambda\,\Delta z}{\gamma\,N^2\,\delta x_0^2}}\cdot\mathbf{F}\cdot\mathbf{Q}_{\frac{(1-\gamma)\,\delta x_0^2}{\lambda\,\Delta z}}\cdot\boldsymbol{u}_{z_0}} \tag{141}$$

where it has been accounted for $\delta\alpha = 1/(N\,\delta x_0)$ according to Eq. (156) and with $\Delta z = z_1 - z_0$.

Note that, taking $\overline{\gamma} = \gamma$ in the 2-step Fresnel propagation in Eq. (131) exactly yields Eq. (141) provided $\Delta z' > 0$ and $\Delta z'' < 0$. The fact that $\Delta z'' = -\overline{\gamma}\,\Delta z'$ warrants that $\Delta z'$ and $\Delta z''$ have opposite signs when $\overline{\gamma} = \gamma > 0$. Check that this does not make any difference because the direct and inverse Fourier transform of the Fresnel propagation kernel are the same, due to its Gaussian structure.

Fractional Fourier transform. **?** proposed to use the fractional Fourier transform (FRFT) to perform Fresnel propagation by the same numerical method in the near and far fields. The resulting general expression, Eq. (18) in their paper, is an instance of the two-step paraxial propagation method.

In **?**, the propagation kernel is approximated by:

$$h_z^{\mathrm{Mas}}(x,y) = \exp\left(\mathrm{i}\,\pi\,\frac{x^2+y^2}{\lambda\,z}\right). \tag{142}$$

which, compared to Eq. (44), omits the factor $\exp(\mathrm{i}\,k\,z)/(\mathrm{i}\,\lambda\,z)$. This factor is needed to take into account the dilution of the amplitude and the optical path delay with the propagation distance z. Accounting for this phase delay may be important for modeling optical setups, such as interferometers, where the wave propagates along different interfering arms.

3 Optical components

Except when explicitly stated, diffraction by planar surfaces under the paraxial conditions (*i.e.* Fresnel diffraction) will be always be assumed.

3.1 Point source

From Eq. (18), a point source at position $\boldsymbol{r}_0 = (x_0, y_0, z_0)$ simply yields a field proportional to $h_{z-z_0}(x - x_0, y - y_0)$ at position $\boldsymbol{r} = (x, y, z)$ with $h_{\Delta z}$ the propagation kernel.

3.2 Thin lens

To model the effects of a thin lens of focal length f (positive for a converging lens, negative for a diverging lens) whose center is at $\boldsymbol{r}_\mathrm{c} = (x_\mathrm{c}, y_\mathrm{c}, z_\mathrm{c})$, we consider its effect on a point source at the front focal point of the lens, hence at position $\boldsymbol{r}_\mathrm{c} - f\,\boldsymbol{e}_z = (x_\mathrm{c}, y_\mathrm{c}, z_\mathrm{c} - f)$. In the transverse plane at z_c and just before the lens, the field is the one produced by the point source (see Section 3.1):

$$u_\mathrm{in}(\boldsymbol{x}) \propto h_f(\boldsymbol{x} - \boldsymbol{x}_\mathrm{c}) \propto \mathrm{e}^{\mathrm{i}\,k\,\frac{\|\boldsymbol{x}-\boldsymbol{x}_\mathrm{c}\|^2}{2\,f}}$$

where paraxial conditions have been assumed. Just after the lens, the wave should be planar, hence the effects of the thin lens is to add or subtract a quadratic phase to the incoming wavefront. The output field (after the lens) is thus given by:

$$u_\mathrm{out}(x, y) = u_\mathrm{in}(x, y)\,\mathrm{e}^{\mathrm{i}\,k\left[\ell - \frac{\|\boldsymbol{x}-\boldsymbol{x}_\mathrm{c}\|^2}{2\,f}\right]} \tag{143}$$

for any input field u_out (before the lens) and with $\ell \geq 0$ an optical path length accounting for the thickness of the lens:

$$\ell = \frac{n_\mathrm{glass}}{n}\,\ell_\mathrm{c} \tag{144}$$

with n and n_glass the respective refractive indices of the propagation medium and of the lens material and where ℓ_c is the physical thickness of the lens at its center.

What if the lens is tilted? Answer: move the point source at the actual position of the focus.

A The field as a superposition of plane waves

It is possible to find a family of solutions of the Helmholtz equation that are separable in Cartesian coordinates $\boldsymbol{r} = (x, y, z)$. Taking $u(x, y, z) = f_x(x)\, f_y(y)\, f_z(z)$ in Eq. (6) and dividing by $u(x, y, z)$, assuming it is not zero, yields:

$$\frac{f_x''(x)}{f_x(x)} + \frac{f_y''(y)}{f_y(y)} + \frac{f_z''(z)}{f_z(z)} + k^2 = 0.$$

In the right-hand side expression, the first term only depends on x, the second term only depends on y, the third term only depends on z, and the fourth term is constant. Hence all these terms must be constant, so that Helmholtz equation amounts to:

$$\begin{cases} f_x''(x) = \rho_x\, f_x(x) \\ f_y''(y) = \rho_y\, f_y(y) \\ f_z''(z) = \rho_z\, f_z(z) \end{cases} \qquad \text{subject to} \quad \rho_x + \rho_y + \rho_z + k^2 = 0$$

with $(\rho_x, \rho_y, \rho_z) \in \mathbb{R}^3$. For a given component, say f_x, the possible solutions depend on the sign of ρ_x:

- If $\rho_x > 0$, introducing $\mu_x = \sqrt{\rho_x} > 0$, the solution is a linear combination of $\exp(\mu_x\, x)$ and of $\exp(-\mu_x\, x)$. These particular solutions are amplified exponentially while they propagate in a direction such that x is respectively increasing or decreasing. This is impossible in the absence of sources. Hence, the only physically possible solution is a linear combination of the exponentially damped particular solutions:

  $$f_x(x) = f_x(x_0)\, \mathrm{e}^{-\mu_x\, |x - x_0|}$$

  which is rapidly vanishing with the distance $|x - x_0|$ and is called an **evanescent wave**.

- If $\rho_x \leq 0$, the solution is a linear combination of $\exp(\mathrm{i}\, k_x\, x)$ with $k_x = \pm\sqrt{-\rho_x}$ so that $k_x^2 = -\rho_x$. In that case, $f_x(x)$ is a sinusoidal function of x with wave number $|k_x|$.

The general solution to the Helmholtz equation (6), that is the field $u(x, y, z)$, is a superposition of all possible particular solutions which, neglecting the evanescent waves, are given by:

$$\mathrm{e}^{\mathrm{i}\,(k_x\, x + k_y\, y + k_z\, z)} \quad \text{such that} \quad k_x^2 + k_y^2 + k_z^2 = k^2. \tag{145}$$

In other words and neglecting the evanescent waves, the field $u(\boldsymbol{r})$ can be written as the superposition of mono-chromatic plane waves propagating as $\exp(\mathrm{i}\, \boldsymbol{k} \cdot \boldsymbol{r})$ with wave vector $\boldsymbol{k} = (k_x, k_y, k_z)$ and such that $\|\boldsymbol{k}\| = k = 2\,\pi/\lambda$. Owing to this latter constraint that holds for a mono-chromatic wave, there are only 2 free parameters out of k_x, k_y, and k_z. For instance, taking $k_z = \pm\sqrt{k^2 - k_x^2 - k_y^2}$, the most general expression for the superposition of the mono-chromatic plane waves is given by:

$$u(x, y, z) = \iint_{\mathcal{D}_k} \left[a(k_x, k_y)\, \mathrm{e}^{+\mathrm{i}\,\sqrt{k^2-k_x^2-k_y^2}\, z} + b(k_x, k_y)\, \mathrm{e}^{-\mathrm{i}\,\sqrt{k^2-k_x^2-k_y^2}\, z}\right] \times \mathrm{e}^{\mathrm{i}\,(k_x\, x + k_y\, y)}\, \mathrm{d}k_x\, \mathrm{d}k_y \tag{146}$$

where $a(k_x, k_y)$ and $b(k_x, k_y)$ are the weights of the superposition and:

$$\mathcal{D}_k = \left\{(k_x, k_y) \in \mathbb{R}^2 \mid k_x^2 + k_y^2 \leq k^2\right\} \tag{147}$$

is the disk of radius k centered at $(0, 0)$.

Note that, in Eq. (146), the choice of the axes of the Cartesian frame are arbitrary and that boundary conditions may apply to yield a more specific expression for the propagating field. See for example Section 1.3.2 "*Angular Spectrum*" where, using the angular spectrum, the very general solution in Eq. (146) can be restricted and simplified if we assume known the field in a plane defined by, say, $z = z_0$.

B The discrete Fourier transform

B.1 Uni-dimensional case

The Fourier transform of $f(x)$ at frequency α is defined by:

$$\widetilde{f}(\alpha) = \int_{-\infty}^{+\infty} f(x)\,\mathrm{e}^{-\mathrm{i}\,2\,\pi\,\alpha\,x}\,\mathrm{d}x. \tag{148}$$

The inverse transform is given by:

$$f(x) = \int_{-\infty}^{+\infty} \widetilde{f}(\alpha)\,\mathrm{e}^{+\mathrm{i}\,2\,\pi\,\alpha\,x}\,\mathrm{d}\alpha. \tag{149}$$

Using N evenly spaced positions $x_j = x_0 + j\,\delta x$ with δx the sampling step and for $j \in \{0, 1, ..., N-1\}$, $\widetilde{f}(\alpha)$ can be approximated by a Riemann sum:

$$\widetilde{f}(\alpha) \approx \sum_{j=0}^{N-1} f(x_j)\,\mathrm{e}^{-\mathrm{i}\,2\,\pi\,\alpha\,x_j}\,|\delta x|. \tag{150}$$

To have an invertible discrete transform, the frequencies α must also be sampled with N samples. Considering a uniform sampling of the frequencies, the discrete frequencies are given by $\alpha_k = \alpha_0 + k\,\delta\alpha$ with $\delta\alpha$ the frequency sampling step and for $k \in \{0, 1, ..., N-1\}$. The sampled spectrum is then given by:

$$\widetilde{f}(\alpha_k) \approx |\delta x| \sum_{j=0}^{N-1} \mathrm{e}^{-\mathrm{i}\,2\,\pi\,\alpha_k\,x_j}\,f(x_j) = |\delta x| \sum_{j=0}^{N-1} F_{k,j}\,f(x_j), \tag{151}$$

with:

$$F_{k,j} = \mathrm{e}^{-\mathrm{i}\,2\,\pi\,\alpha_k\,x_j}. \tag{152}$$

Hence $|\delta x|\,\mathbf{F}$ is a linear operator implementing a discrete approximation of the continuous Fourier transform.

Following the same reasoning to approximate the inverse Fourier transform of $\widetilde{f}(\alpha)$ which yields $f(x)$, the inverse discrete Fourier transform should be implemented by $|\delta\alpha|\,\mathbf{F}^\star$ with $\mathbf{F}^\star$ the adjoint, that is the conjugate transpose, of $\mathbf{F}$ and $\delta\alpha$ the frequency sampling step. For $|\delta\alpha|\,\mathbf{F}^\star$ to really be the inverse of $|\delta x|\,\mathbf{F}$, the following conditions must hold:

$$|\delta x\,\delta\alpha|\,\big(\mathbf{F}^\star \cdot \mathbf{F}\big)_{j,k} = \begin{cases} 1 & \text{if } j = k, \\ 0 & \text{else.} \end{cases} \tag{153}$$

Expanding the left-hand side of this equation yields:

$$
\begin{aligned}
|\delta x\,\delta\alpha|\,\big(\mathbf{F}^\star\cdot\mathbf{F}\big)_{j,k} &= |\delta x\,\delta\alpha|\sum_{\ell=0}^{N-1} F^\star_{j,\ell}\,F_{\ell,k} \\
&= |\delta x\,\delta\alpha|\sum_{\ell=0}^{N-1} \mathrm{e}^{\mathrm{i}\,2\,\pi\,\alpha_\ell\,(x_j-x_k)} \\
&= |\delta x\,\delta\alpha|\,\mathrm{e}^{\mathrm{i}\,2\,\pi\,\alpha_0\,(j-k)\,\delta x}\sum_{\ell=0}^{N-1} \mathrm{e}^{\mathrm{i}\,2\,\pi\,\delta\alpha\,\delta x\,(j-k)\,\ell} \\
&= |\delta x\,\delta\alpha|\,\mathrm{e}^{\mathrm{i}\,2\,\pi\,\alpha_0\,(j-k)\,\delta x}\begin{cases} N & \text{if } \psi=1 \\ \frac{1-\psi^N}{1-\psi} & \text{else}\end{cases}
\end{aligned}
\tag{154}
$$

We first assume that $j = k$, then all complex exponential terms in the right-hand side of Eq. (154) are equal to 1 and thus the first condition in Eq. (153) amounts to $N\,|\delta x\,\delta\alpha| = 1$. Using this result and assuming now that $j \neq k$, the second condition in Eq. (153) imposes that the sum in the right-hand side of Eq. (154) be equal to 0:

$$
0 = \sum_{\ell=0}^{N-1} \mathrm{e}^{\mathrm{i}\,2\,\pi\,(j-k)\,\ell/N} = \sum_{\ell=0}^{N-1} \psi^\ell = \begin{cases} N & \text{if } \psi=1 \\ \frac{1-\psi^N}{1-\psi} & \text{else}\end{cases}
\tag{155}
$$

with $\psi = \mathrm{e}^{\pm\mathrm{i}\,2\,\pi\,(j-k)/N}$ and where $\pm$ is the sign of $\delta x\,\delta\alpha$. When $j \neq k$, $0 < |j-k| < N$ holds, it follows that $\psi \neq 1$ and thus that the above sum is equal to $(1-\psi^N)/(1-\psi)$. Now, since $j-k$ is integer, $\psi^N = 1$ whatever the values of j and k and the sum is thus equal to 0 as required.

To summarize, it is sufficient that the sampling condition $N\,|\delta x\,\delta\alpha| = 1$ holds to have $|\delta x|\,\mathbf{F}$ and $|\delta\alpha|\,\mathbf{F}^\star$ implement discrete approximation of the continuous Fourier transform and of its inverse. However, in order to have the signs in the complex exponents of the entries of $\mathbf{F}$ be the same as in the continuous version (as in Eq. (157) below), the sampling steps must have the same signs and the sampling condition writes:

$$
N\,\delta x\,\delta\alpha = 1. \tag{156}
$$

The coefficients of $\mathbf{F}$ are then given by:

$$
F_{j,k} = \mathrm{e}^{-\mathrm{i}\,2\,\pi\,j\,k/N}. \tag{157}
$$

Due to the sampling condition, the magnitude of the highest sampled frequency, the so-called **Nyquist frequency**, is (for an even number N of samples):

$$
\alpha_{\mathrm{max}} = \frac{N}{2}\,|\delta\alpha| = \frac{1}{2\,|\delta x|} \tag{158}
$$

as stated by Whittaker-Shannon theorem. In implementations of the discrete Fourier transform (DFT), it is usually assumed that the first sample is at the origin in the direct and in the conjugate spaces, hence:

$$
\begin{aligned}
x_0 &= 0 \\
\alpha_0 &= 0
\end{aligned}
\tag{159}
$$

by convention, not by necessity.

B.2 Multi-dimensional case

The results found for the uni-dimensional DFT can be generalized to d-dimensional DFT as follows.

The direct space is sampled on a $N_1 \times N_2 \times \ldots \times N_d$ Cartesian grid with sampling steps δx_1, δx_2, ..., and δx_d along the axes. The sampling condition given in Eq. (156) for the frequency step applies separately along each dimension $i \in \{1, 2, \ldots, d\}$:

$$N_i \, \delta x_i \, \delta \alpha_i = 1. \tag{160}$$

Using d-dimensional Cartesian indices $\boldsymbol{j} = (j_1, j_2, \ldots, j_d)$ and $\boldsymbol{k} = (k_1, k_2, \ldots, j_d)$, the coefficients of the direct DFT operator are given by:

$$F_{\boldsymbol{k},\boldsymbol{j}} = \mathrm{e}^{-\mathrm{i}\, 2\, \pi \, \langle\langle \boldsymbol{j}, \boldsymbol{k} \rangle\rangle} \tag{161}$$

with:

$$\langle\langle \boldsymbol{j}, \boldsymbol{k} \rangle\rangle = \sum_{i=1}^{d} \frac{j_i \, k_i}{N_i} \tag{162}$$

and the inverse of the DFT operator $\mathbf{F}$ is:

$$\mathbf{F}^{-1} = \frac{1}{\prod_{i=1}^{d} N_i} \, \mathbf{F}^{\star} \tag{163}$$

where $\mathbf{F}^{\star}$ is the adjoint, that is the conjugate transpose, of $\mathbf{F}$.

Equipped with this estimator, the continuous d-dimensional Fourier transform and its inverse may be approximated by:

$$\mathbb{F} = \left(\prod_{i=1}^{d} |\delta x_i| \right) \mathbf{F}, \tag{164}$$

$$\mathbb{F}^{-1} = \left(\prod_{i=1}^{d} |\delta \alpha_i| \right) \mathbf{F}^{\star} = \frac{1}{\prod_{i=1}^{d} N_i \, |\delta x_i|} \, \mathbf{F}^{\star}, \tag{165}$$